

Distributed Binary Detection over Fading Channels: Cooperative and Parallel Architectures

Nahal Maleki[†], *IEEE Student Member*, Azadeh Vosoughi[‡], *IEEE Senior Member*,
Nazanin Rahnavard[‡], *IEEE Member*

Abstract

This paper considers the problem of binary distributed detection of a known signal in correlated Gaussian sensing noise in a wireless sensor network, where the sensors are restricted to use likelihood ratio test (LRT), and communicate with the fusion center (FC) over bandwidth-constrained channels that are subject to fading and noise. To mitigate the deteriorating effect of fading encountered in the conventional parallel fusion architecture, in which the sensors directly communicate with the FC, we propose new fusion architectures that enhance the detection performance, via harvesting cooperative gain (so-called “decision diversity gain”). In particular, we propose: (i) cooperative fusion architecture with Alamouti’s space-time coding (STC) scheme at sensors, (ii) cooperative fusion architecture with signal fusion at sensors, and (iii) parallel fusion architecture with local threshold changing at sensors. For these schemes, we derive the LRT and majority fusion rules at the FC, and provide upper bounds on the average error probabilities for homogeneous sensors, subject to uncorrelated Gaussian sensing noise, in terms of signal-to-noise ratio (SNR) of communication and sensing channels. Our simulation results indicate that, when the FC employs the LRT rule, unless for low communication SNR and moderate/high sensing SNR, performance improvement is feasible with the new fusion architectures. When the FC utilizes the majority rule, such improvement is possible, unless for high sensing SNR.

Copyright (c) 2015 IEEE. Personal use of this material is permitted. However, permission to use this material for any other purposes must be obtained from the IEEE by sending a request to pubs-permissions@ieee.org.

This work is supported by National Science Foundation under Grant CCF-1336123, CCF-1341966, ECCS-1056065 and CCF-0915994. Part of this work is presented in SPAWC 2009 [19]

[†]N. Maleki is with the ECE Department, University of Rochester, Rochester, NY (e-mail: nmalekit@ur.rochester.edu). [‡]A. Vosoughi is with the EECS Department, University of Central Florida, Orlando, FL (e-mail: azadeh@ucf.edu). [‡]N. Rahnavard is with the EECS Department, University of Central Florida, Orlando, FL (e-mail: nazanin@eeecs.ucf.edu).

Distributed Detection, Parallel Architecture, Fusion and Sensor Rule, Correlation, Space-Time Coding, Diversity, Error Floor

I. INTRODUCTION

The problem of distributed detection with the fusion center (FC) (so-called classical parallel fusion architecture) has a long and rich history, where each local detector (sensor) processes its observation locally and independently, and passes its local binary decision to the FC. The main assumption in the classical works is that the bandwidth-constrained communication channels are *error-free* and thus the reliability of the final decision at the FC is determined by the reliability of the local binary decisions. However, wireless channels are inherently error-prone, due to noise and fading. An *integrated approach* of distributed detection over noisy fading channels was considered in [1]–[12], in which the sensors send their modulated local binary decisions to the FC and the FC employs a fusion rule, incorporating channel state information (CSI), to improve the reliability of the final decision at the FC. The performance of these integrated distributed detection is ultimately limited by the communication bounds. A common thread in the schemes discussed in [1]–[12] is that they are non-cooperative, i.e., there is no information exchange among the sensors. Cooperative wireless communication [13], [18] has been proven to significantly enhance performance in the presence of fading, via invoking spatial diversity, that leads into mitigation of the detrimental fading effects [13], [18]. Motivated by the promises of cooperative communication, we propose a new class of integrated distributed detection, which harvests cooperative gain (enabled by at most 1-bit information exchange among one-hop neighboring nodes) and improves the performance of the integrated distributed detection [1], [2] in the presence of fading, via allowing each sensor to send (at most) 2 information bits to the FC and assuming identical transmit power per node. In particular, we propose three schemes: (i) cooperative fusion architecture with Alamouti’s space-time coding (STC) scheme at sensors, in which neighboring sensors exchange 1 information bit and each sensor sends 2 information bits to the FC; (ii) cooperative fusion architecture with signal fusion at sensors, in which neighboring sensors exchange 1 information bit and each sensor sends 1 information bit to the FC; and (iii) parallel fusion architecture with local threshold changing at sensors, in which neighboring sensors do not exchange information and each sensor sends 2 information bits to the FC. To describe the proposed schemes, suppose \mathcal{S}_1 and \mathcal{S}_2 are two designated cooperative partners. *In scheme (i)*, rather

than transmitting their local decisions directly to the FC, \mathcal{S}_1 and \mathcal{S}_2 are coordinated to form a transmit cluster, such that they first exchange their local decisions and apply Alamouti's scheme [19], [20] for transmitting the decisions to the FC. Different from most literature on distributed STC, which assume a node acts as a relay only for error-free reception [21], we consider the fact that the channels between \mathcal{S}_1 and \mathcal{S}_2 are subject to errors, due to noise and fading. *In scheme (ii)*, similar to scheme (i), \mathcal{S}_1 and \mathcal{S}_2 exchange their local decisions. Instead of applying Alamouti's scheme, however, each node updates its decision, via optimally fusing its observation with the received signal from its cooperative partner. Updated decisions are transmitted to the FC. *In scheme (iii)*, different from schemes (i) and (ii), there is no explicit information exchange between \mathcal{S}_1 and \mathcal{S}_2 . Each node forms two decisions, where one is made based on its observation only and the other is obtained based on optimally fusing its observation with its guess of the decision of its cooperative partner. \mathcal{S}_1 and \mathcal{S}_2 apply Alamouti's scheme for transmitting these decisions to the FC. For these three schemes we provide the likelihood ratio test (LRT) and majority fusion rules at the FC. The average (over fading) error probability of decision error at the FC for these schemes depend on signal-to-noise ratio (SNR) of communication (channels between cooperative partners as well as between the nodes and the FC) and sensing channels (channels between the target and the nodes). For the proposed schemes we derive upper bounds on the average error probability and investigate how a node should allocate its transmit power for communicating with its cooperative partner and the FC, such that the error is minimized. These results enable us to quantify the cooperative gain offered by the proposed schemes, with respect to the schemes in [1], [2], assuming identical transmit power per node.

Information exchange among the nodes for *consensus-based* distributed detection without the FC has been studied before (examples are [14]–[17]). [14]–[16] considered a consensus-based distributed detection system, where the sensors successively update and broadcast their local binary decisions over *error-free* links [14]–[16]. In [17] each sensor successively updates its continuous-valued decision variable and passes it to its neighbors over random links without bandwidth constraint. Distributed detection in networks *with feedback* has been studied before (examples are [23]–[25]) from information theoretic perspective, focusing on the asymptotic regime (i.e., networks with large number of sensors) and quantifying performance in terms of error exponents. These works consider a variety of feedback architectures, including two-message feedback architectures, where each sensor sends its first message to the FC, based on its own observation, and sends its second message, based on the additional information

provided by the FC through feedback, where the feedback contains (functions of) the messages generated⁴ by (some) other sensors. Different from these works, we consider networks with a finite number of sensors, without feedback from the FC, where (at most) 1-bit information exchange is allowed between two cooperative sensors. Also, we relax the error-free communication constraint, by considering fading effects during the information exchange phase, i.e., we assume a sensor knows the decision of its partner with a limited reliability, that is dictated by the quality of inter-sensor communication channel. Perhaps the most related work is [22], in which each sensor communicates its local binary decision to its neighbors and the sensors communicate their updated binary decisions to the FC. The local decision rules and the fusion rule at the FC are *all majority rules* and communication channels are assumed to be *error-free* in [22]. To the best of our knowledge, for parallel fusion architecture no prior work has studied the impact of local (limited) information exchange on enhancing the performance of the integrated distributed detection systems [1]–[12] operating in a noisy fading environment. Paper organization follows. Section II introduces our sensing model and overviews the integrated distributed detection schemes in [1], [2] for this work to be self-explanatory. Sections III, IV, V describe schemes (i),(ii),(iii), respectively, and provide local decision and fusion rules at the sensors and the FC. Section VI provides the performance analysis. Our numerical results are presented in Section VII. Concluding remarks are in Section VIII.

II. BASIC MODELS

A. Sensing Model

We consider the binary hypothesis testing problem of detecting a known signal in correlated Gaussian noise based on measurements x_k at K distributed sensors. The *a priori* probabilities of two hypotheses $\mathcal{H}_0, \mathcal{H}_1$ are denoted by π_0, π_1 , respectively. The FC is tasked with determining whether the unknown hypothesis is \mathcal{H}_0 or \mathcal{H}_1 , based on the information collected from the K sensors. The measurement x_k of sensor \mathcal{S}_k under \mathcal{H}_0 and \mathcal{H}_1 , respectively, are $x_k = w_k$ and $x_k = 1 + w_k$ for $k = 1, \dots, K$, where sensing noise w_k is zero-mean with variance $\sigma_{w_k}^2$. The spatial correlation between noises w_i, w_j are characterized with the correlation coefficient ρ_{ij} . We assume sensors are grouped into $S = K/2$ distinct pairs of cooperative partners $(\mathcal{S}_i, \mathcal{S}_j)$, where \mathcal{S}_i knows $\sigma_{w_i}^2, \sigma_{w_j}^2$ and ρ_{ij} only and is restricted to use LRT. The FC employs LRT, when all sensing noise variances and pairwise correlation coefficients are available at the FC. In the absence of this knowledge, the FC uses the majority rule.

B. Classical Parallel Fusion Architecture

Each sensor \mathcal{S}_k makes a local binary decision $u_k \in \{1, -1\}$ based on its measurement x_k . The local decisions $+1$ and -1 correspond to the hypotheses \mathcal{H}_1 and \mathcal{H}_0 , respectively. The local detection performance of \mathcal{S}_k are characterized with $P_{d_k} = P(u_k = 1|\mathcal{H}_1)$ and $P_{f_k} = P(u_k = 1|\mathcal{H}_0)$. To form u_k , sensor \mathcal{S}_k applies the LRT $\frac{f(x_k|\mathcal{H}_1)}{f(x_k|\mathcal{H}_0)} \underset{u_k=-1}{\overset{u_k=1}{\geq}} \frac{\pi_0}{\pi_1}$. For the sensing model in Section II-A,

the LRT is reduced to $x_k \underset{u_k=-1}{\overset{u_k=1}{\geq}} \tau_k$ where $\tau_k = 0.5 + \sigma_{w_k}^2 \ln(\frac{\pi_0}{\pi_1})$. Also, $P_{d_k} = Q(\frac{\tau_k - 1}{\sigma_{w_k}})$ and $P_{f_k} = Q(\frac{\tau_k}{\sigma_{w_k}})$, where $Q(x)$ denotes the Q -function¹. The local decisions u_k are transmitted over

orthogonal channels subject to noise and fading to the FC. When \mathcal{S}_k sends u_k the received signal at the FC is $y_k = u_k h_k + v_k$ where $h_k \sim \mathcal{CN}(0, \sigma_{h_k}^2)$, $v_k \sim \mathcal{CN}(0, \sigma_v^2)$. where h_k represents the fading channel coefficient corresponding to the channel between \mathcal{S}_k and the FC. The channel variance is $\sigma_{h_k}^2 = \mathcal{P}\mathcal{G}/d_k^\varepsilon$, where \mathcal{P} represents transmit power of \mathcal{S}_k , d_k denotes the distance between \mathcal{S}_k and the FC, ε is the pathloss exponent, and \mathcal{G} is a constant that depends on the antenna gains and the wavelength. We

assume that ε and \mathcal{G} are identical for all links. The term v_k is the receiver noise at the FC. We assume v_k and h_k are independent. We define $\bar{\gamma}_{h_k}^2 = \frac{\sigma_{h_k}^2}{\sigma_v^2}$ as the average received SNR corresponding to node \mathcal{S}_k -FC communication channel. Relying on the received signals y_k and the availability of CSI h_k the

FC forms the LRT $\Lambda = \frac{f(y_1, \dots, y_K|\mathcal{H}_1)}{f(y_1, \dots, y_K|\mathcal{H}_0)}$, where $f(y_1, \dots, y_K|\mathcal{H}_\ell)$ indicates the joint pdf of y_1, \dots, y_K given the hypothesis \mathcal{H}_ℓ , to make the final decision. In particular, the FC decides \mathcal{H}_1 when $\Lambda > \pi_0/\pi_1$ and decides \mathcal{H}_0 otherwise. Considering that $\mathcal{H}_\ell \rightarrow u_1, \dots, u_K \rightarrow y_1, \dots, y_K$ form a Markov chain and also the fact $f(y_1, \dots, y_K|u_1, \dots, u_K) = \prod_{k=1}^K f(y_k|u_k)$ we can simplify Λ as follows

$$\Lambda = \frac{\sum_{u_1} \dots \sum_{u_K} \left(\prod_{k=1}^K f(y_k|u_k) \right) P(u_1, \dots, u_K|\mathcal{H}_1)}{\sum_{u_1} \dots \sum_{u_K} \left(\prod_{k=1}^K f(y_k|u_k) \right) P(u_1, \dots, u_K|\mathcal{H}_0)}. \quad (1)$$

Focusing on the terms $f(y_k|u_k)$ in (1) we note that given h_k, u_k we have $y_k \sim \mathcal{CN}(u_k h_k, \sigma_v^2)$. Considering the term $P(u_1, \dots, u_K|\mathcal{H}_\ell)$ in (1) we note that it depends on the characteristics of the sensing channel noises described in Section II-A. When Gaussian sensing noises are uncorrelated $\rho_{ij} = 0$ for all $i \neq j$,

¹Considering the local LRT at sensor k , the distributions $f(x_k|\mathcal{H}_\ell)$ for $\ell = 0, 1$ and P_{d_k}, P_{f_k} values depend on the distribution of sensing noises. Thus the simplified form of the local rule and P_{d_k}, P_{f_k} expressions would change for non-Gaussian w_k . Given the joint pdf $f(w_1, \dots, w_K)$ at the FC, the expressions Λ in (1) for dependent and (2) for independent w_k 's remain unchanged.

this term is simplified to $\prod_{k=1}^K P(u_k|\mathcal{H}_\ell)$ and (1) is reduced to [1], [2]

$$\Lambda = \prod_{k=1}^K \frac{P_{d_k} f(y_k|u_k = 1) + (1 - P_{d_k}) f(y_k|u_k = -1)}{P_{f_k} f(y_k|u_k = 1) + (1 - P_{f_k}) f(y_k|u_k = -1)}. \quad (2)$$

When the parameters of sensing channels are unavailable at the FC, the FC cannot apply the optimal LRT in (1) or (2). Alternatively, the FC demodulates the channel inputs u_k using y_k for $k = 1, \dots, K$ and applies the majority rule to the demodulated symbols to reach the final decision, i.e., if the sum of the demodulated symbols is positive the FC decides \mathcal{H}_1 and otherwise decides \mathcal{H}_0 .

III. COOPERATIVE FUSION ARCHITECTURE WITH STC AT SENSORS

A. Inter-node Communication Channel Model and Local Decision Rules at Sensors

Suppose nodes \mathcal{S}_i and \mathcal{S}_j are within a pair, that is \mathcal{S}_i and \mathcal{S}_j are cooperative partners. Each sensor makes a decision based on its measurement. The nodes exchange their decisions over orthogonal channels subject to noise and fading. Let u_i denote the decision made at \mathcal{S}_i based on x_i . Sensor \mathcal{S}_i transmits $\sqrt{1 - \alpha}u_i$, where $0 < \alpha < 1$ is a power normalization factor, to assure that the total transmit power of nodes in this architecture remains the same as that of the classical parallel fusion architecture in Section II-B. When \mathcal{S}_i transmits $\sqrt{1 - \alpha}u_i$ the received signal at \mathcal{S}_j is

$$r_{ij} = \sqrt{1 - \alpha}u_i g_{ij} + \eta_{ij} \quad \text{where} \quad g_{ij} \sim \mathcal{CN}(0, \sigma_{hs_{ij}}^2), \quad \eta_{ij} \sim \mathcal{CN}(0, \sigma_\eta^2). \quad (3)$$

g_{ij} represents fading channel coefficient from \mathcal{S}_i to \mathcal{S}_j and η_{ij} is receiver noise at \mathcal{S}_j . The channel variance is $\sigma_{hs_{ij}}^2 = \mathcal{P}\mathcal{G}/d_{ij}^\epsilon$, where d_{ij} denotes the distance between \mathcal{S}_i and \mathcal{S}_j . Noises η_{ij} , η_{ji} and channel coefficients g_{ij} , g_{ji} are independent and noises are independent and identically distributed (i.i.d.) across all pairs. Upon receiving r_{ij} , \mathcal{S}_j demodulates the channel input u_i , using the knowledge of g_{ij}

$$\hat{u}_i = \text{sgn}(\Re(r_{ij}/g_{ij})). \quad (4)$$

The pair $(\mathcal{S}_i, \mathcal{S}_j)$ sends the information $u_i, \hat{u}_i, u_j, \hat{u}_j$ to the FC in two consecutive time slots, exploiting Alamouti's STC scheme. In particular, in the n th slot, \mathcal{S}_i and \mathcal{S}_j send simultaneously $\sqrt{\frac{\alpha}{2}}u_i$ and $\sqrt{\frac{\alpha}{2}}u_j$, respectively. In the $(n + 1)$ th time slot, \mathcal{S}_i and \mathcal{S}_j send simultaneously $-\sqrt{\frac{\alpha}{2}}\hat{u}_j$ and $\sqrt{\frac{\alpha}{2}}\hat{u}_i$, respectively. Considering the definitions of channel variances, we note that effectively \mathcal{S}_i spends $(1 - \alpha)\mathcal{P}$ and $\alpha\mathcal{P} = \frac{\alpha}{2}\mathcal{P} + \frac{\alpha}{2}\mathcal{P}$, respectively, for inter-node and sensor-FC communication.

B. Node-FC Communication Channel Model and Fusion Rule at the FC

Let $y_{ij}(n)$ and $y_{ij}(n+1)$ denote the received signals at the FC corresponding to the pair $(\mathcal{S}_i, \mathcal{S}_j)$ during two consecutive time slots. We have

$$y_{ij}(n) = \sqrt{\frac{\alpha}{2}}(u_i h_i + u_j h_j) + v_{ij}(n), \quad y_{ij}(n+1) = \sqrt{\frac{\alpha}{2}}(-\hat{u}_j h_i + \hat{u}_i h_j) + v_{ij}(n+1)$$

where $h_i \sim \mathcal{CN}(0, \sigma_{h_i}^2)$, $h_j \sim \mathcal{CN}(0, \sigma_{h_j}^2)$, $v_{ij}(n), v_{ij}(n+1) \sim \mathcal{CN}(0, \sigma_v^2)$. (5)

The term $v_{ij}(n)$ is the receiver noise at the FC during the n th time slot. We assume noises $v_{ij}(n), v_{ij}(n+1)$ and channel coefficients h_i, h_j are independent and noises are i.i.d. across all pairs. Taking a similar processing as the Alamouti decoding [20], the FC first forms z_i, z_j using $y_{ij}(n), y_{ij}^*(n+1)$ as follows

$$\begin{aligned} \begin{bmatrix} z_i \\ z_j \end{bmatrix} &= \begin{bmatrix} h_i^* & h_j \\ h_j^* & -h_i \end{bmatrix} \begin{bmatrix} y_{ij}(n) \\ y_{ij}^*(n+1) \end{bmatrix} = \begin{bmatrix} h_i^* & h_j \\ h_j^* & -h_i \end{bmatrix} \begin{bmatrix} v_{ij}(n) \\ v_{ij}^*(n+1) \end{bmatrix} \\ &+ \sqrt{\frac{\alpha}{2}} \left(\begin{bmatrix} |h_i|^2 & h_j h_i^* \\ h_i h_j^* & |h_j|^2 \end{bmatrix} \begin{bmatrix} u_i \\ u_j \end{bmatrix} + \begin{bmatrix} |h_j|^2 & -h_j h_i^* \\ -h_i h_j^* & |h_i|^2 \end{bmatrix} \begin{bmatrix} \hat{u}_i \\ \hat{u}_j \end{bmatrix} \right). \end{aligned}$$

Note that if each node allocates equal power for communicating with its cooperative partner and with the FC, i.e., $\alpha = 1/2$ and also there is no error during inter-node communication, i.e., $\hat{u}_i = u_i, \hat{u}_j = u_j$, the above equations reduce to the classical Alamouti's scheme [20]. The new noise terms $\delta_{ij}^1 = h_i^* v_{ij}(n) + h_j v_{ij}^*(n+1)$ and $\delta_{ij}^2 = h_j^* v_{ij}(n) - h_i v_{ij}^*(n+1)$ are i.i.d. zero mean complex Gaussian RVs with the variance $\sigma^2 = (|h_i|^2 + |h_j|^2) \sigma_v^2$. Next, using the signals z_i, z_j and the CSI h_i, h_j for all pairs the FC forms the LRT $\Lambda = \frac{f(z_i, z_j \text{ for all pairs} | \mathcal{H}_1)}{f(z_i, z_j \text{ for all pairs} | \mathcal{H}_0)}$, where $f(z_i, z_j \text{ for all pairs} | \mathcal{H}_\ell)$ indicates the joint pdf of z_i, z_j corresponding to all pairs given the hypothesis \mathcal{H}_ℓ , to make the final decision. In particular, the FC decides on \mathcal{H}_1 when $\Lambda > \pi_0/\pi_1$ and decides on \mathcal{H}_0 otherwise. We note $\mathcal{H}_\ell \rightarrow u_i, u_j, \hat{u}_i, \hat{u}_j \rightarrow z_i, z_j$ and $\mathcal{H}_\ell \rightarrow u_i, u_j \rightarrow \hat{u}_i, \hat{u}_j$ form Markov chains. Also, (z_i, z_j) are independent across the pairs given $u_i, u_j, \hat{u}_i, \hat{u}_j$ for all pairs. Furthermore, given u_i, u_j for for all pairs, (\hat{u}_i, \hat{u}_j) are independent across the

pairs. Therefore, we write

$$\begin{aligned}
f(z_i, z_j \text{ for all pairs} | \mathcal{H}_\ell) &= \sum_{u_i} \sum_{u_j} \sum_{\hat{u}_i} \sum_{\hat{u}_j} f(z_i, z_j \text{ for all pairs} | u_i, u_j, \hat{u}_i, \hat{u}_j \text{ for all pairs}) \\
&\times P(u_i, u_j, \hat{u}_i, \hat{u}_j \text{ for all pairs} | \mathcal{H}_\ell) \\
&= \sum_{u_i} \sum_{\hat{u}_i} \sum_{u_j} \sum_{\hat{u}_j} \left(\prod_{\text{for all pairs}} f(z_i, z_j | u_i, u_j, \hat{u}_i, \hat{u}_j \text{ for } (\mathcal{S}_i, \mathcal{S}_j)) P(\hat{u}_i | u_i \text{ for } (\mathcal{S}_i, \mathcal{S}_j)) P(\hat{u}_j | u_j \text{ for } (\mathcal{S}_i, \mathcal{S}_j)) \right) \\
&\times P(u_i, u_j \text{ for all pairs} | \mathcal{H}_\ell), \tag{6}
\end{aligned}$$

where the sums are taken over all values that $u_i, u_j, \hat{u}_i, \hat{u}_j$ can assume. Focusing on $f(z_i, z_j | u_i, u_j, \hat{u}_i, \hat{u}_j \text{ for } (\mathcal{S}_i, \mathcal{S}_j))$ in (6) we realize that z_i, z_j are conditionally independent complex Gaussian RVs with the variance $\sigma^2 = (|h_i|^2 + |h_j|^2)\sigma_v^2$ and the means μ_i, μ_j given below

$$\mu_i = \sqrt{\frac{\alpha}{2}} (|h_i|^2 u_i + h_j h_i^* u_j + |h_j|^2 \hat{u}_i - h_j h_i^* \hat{u}_j), \quad \mu_j = \sqrt{\frac{\alpha}{2}} (h_i h_j^* u_i + |h_j|^2 u_j - h_i h_j^* \hat{u}_i + |h_i|^2 \hat{u}_j). \tag{7}$$

Focusing on the term $P(\hat{u}_i | u_i \text{ for } (\mathcal{S}_i, \mathcal{S}_j))$ in (6) and considering (4) one can easily verify the following, assuming that the FC only knows the statistics of inter-node channels g_{ij}, g_{ji} [23]

$$P(\hat{u}_i \neq u_i | u_i) = 1 - P(\hat{u}_i = u_i | u_i) = \frac{1}{2} \left(1 - \sqrt{\frac{\bar{\gamma}_{hs_{ij}}}{1 + \bar{\gamma}_{hs_{ij}}}} \right) \quad \text{where} \quad \bar{\gamma}_{hs_{ij}} = \frac{(1 - \alpha)\sigma_{hs_{ij}}^2}{\sigma_\eta^2} \tag{8}$$

denotes the average received SNR corresponding to $(\mathcal{S}_i, \mathcal{S}_j)$ inter-node communication. The term $P(u_i, u_j \text{ for all pairs} | \mathcal{H}_\ell)$ in (6) can be found in terms of the probability of x_i, x_j being in certain intervals for all pairs. For instance, $P(u_i = 1, u_j = -1 \text{ for all pairs} | \mathcal{H}_\ell) = P(x_i > \tau_i, x_j < \tau_j \text{ for all pairs} | \mathcal{H}_\ell)$. These probabilities can be characterized for the sensing channel model in Section II-A, where x_i, x_j are jointly correlated Gaussian RVs with known statistics². When Gaussian sensing noises are uncorrelated we obtain $P(u_i = 1, u_j = -1 \text{ for all pairs} | \mathcal{H}_0) = \prod_{\{i:u_i=1\}} P_{f_i} \prod_{\{j:u_j=-1\}} (1 - P_{f_j})$ or $P(u_i = 1, u_j = -1 \text{ for all pairs} | \mathcal{H}_1) = \prod_{\{i:u_i=1\}} P_{d_i} \prod_{\{j:u_j=-1\}} (1 - P_{d_j})$. When the parameters of sensing channels are unavailable at the FC, the FC cannot apply the LRT. Alternatively, the FC demodulates the channel inputs for all pairs using the signals z_i, z_j for all pairs and applies the majority rule to the demodulated symbols to reach the final decision.

²For non-Gaussian w_k 's, the probability $P(u_i, u_j \text{ for all pairs} | \mathcal{H}_\ell)$ should be calculated in terms of the joint pdf $f(w_1, \dots, w_K)$.

IV. COOPERATIVE FUSION ARCHITECTURE WITH SIGNAL FUSION AT SENSORS

A. Inter-node Communication Channel Model and Local Decision Rules at Sensors

Suppose nodes \mathcal{S}_i and \mathcal{S}_j are within a pair. Each sensor makes an initial decision based on its measurement. The nodes exchange their decisions over orthogonal channels subject to noise and fading. Let u_i denote the decision made at \mathcal{S}_i based on x_i . When \mathcal{S}_i transmits $\sqrt{1-\alpha}u_i$ the received signal at \mathcal{S}_j is r_{ij} as shown in (3). Upon receiving r_{ij} , \mathcal{S}_j (rather than demodulating the channel input) updates its initial decision by fusing r_{ij} and its measurement x_j . In particular, \mathcal{S}_j forms a local LRT $\tilde{\lambda}_j = \frac{f(r_{ij}, x_j | \mathcal{H}_1)}{f(r_{ij}, x_j | \mathcal{H}_0)}$, where $f(r_{ij}, x_j | \mathcal{H}_\ell)$ indicates the joint pdf of r_{ij}, x_j given the hypothesis \mathcal{H}_ℓ , to make a new decision \tilde{u}_j . Node \mathcal{S}_j lets $\tilde{u}_j = 1$ when $\tilde{\lambda}_j > \pi_0/\pi_1$ and lets $\tilde{u}_j = -1$ otherwise. Since $\mathcal{H}_\ell \rightarrow u_i \rightarrow r_{ij}$ and $x_j \rightarrow \mathcal{H}_\ell, u_i \rightarrow r_{ij}$ form Markov chains, we find

$$\tilde{\lambda}_j = \frac{\sum_{u_i} f(r_{ij}|u_i)P(u_i|x_j, \mathcal{H}_1)f(x_j|\mathcal{H}_1)}{\sum_{u_i} f(r_{ij}|u_i)P(u_i|x_j, \mathcal{H}_0)f(x_j|\mathcal{H}_0)}. \quad (9)$$

Considering $f(r_{ij}|u_i)$ in (9) we note that given g_{ij}, u_i we have $r_{ij} \sim \mathcal{CN}(\sqrt{1-\alpha}u_i g_{ij}, \sigma_\eta^2)$. To find $P(u_i|x_j, \mathcal{H}_\ell)$ in (9) we note that for the sensing model in Section II-A, x_i, x_j are jointly Gaussian RVs with the mean ℓ , the variances $\sigma_{w_i}^2, \sigma_{w_j}^2$ and the correlation coefficient $\rho_{i,j}$ under the hypothesis \mathcal{H}_ℓ . Using the joint pdf of x_i, x_j and the Bayes' rule $P(u_i = 1|x_j, \mathcal{H}_\ell) = \frac{P(u_i=1, x_j|\mathcal{H}_\ell)}{f(x_j|\mathcal{H}_\ell)}$ one can show

$$P(u_i = 1|x_j, \mathcal{H}_\ell) = 1 - P(u_i = -1|x_j, \mathcal{H}_\ell) = Q\left(\frac{\tau_i - \rho_{i,j}x_j \frac{\sigma_{w_i}}{\sigma_{w_j}} - \ell(1 - \rho_{i,j} \frac{\sigma_{w_i}}{\sigma_{w_j}})}{\sqrt{(1 - \rho_{i,j}^2)\sigma_{w_i}}}\right). \quad (10)$$

At last, we find $f(x_j|\mathcal{H}_\ell)$ in (9) by noting that given \mathcal{H}_ℓ , we have $x_j \sim \mathcal{CN}(\ell, \sigma_{w_j}^2)$. When Gaussian sensing noises are uncorrelated u_i and x_j are independent³ for a given hypothesis \mathcal{H}_ℓ , leading into $P(u_i|x_j, \mathcal{H}_\ell) = P(u_i|\mathcal{H}_\ell)$. The pair $(\mathcal{S}_i, \mathcal{S}_j)$ sends $\sqrt{\alpha}\tilde{u}_i, \sqrt{\alpha}\tilde{u}_j$ to the FC over two orthogonal channels subject to noise and fading. Considering the definitions of channel variances, we note that effectively \mathcal{S}_i spends $(1-\alpha)\mathcal{P}$ and $\alpha\mathcal{P}$, respectively, for inter-node and sensor-FC communication.

B. Node-FC Communication Channel Model and Fusion Rule at the FC

Let y_i and y_j denote the received signals at the FC corresponding to the pair $(\mathcal{S}_i, \mathcal{S}_j)$. We have

$$y_i = \sqrt{\alpha}\tilde{u}_i h_i + v_i, \quad y_j = \sqrt{\alpha}\tilde{u}_j h_j + v_j, \quad h_i \sim \mathcal{CN}(0, \sigma_{h_i}^2), \quad h_j \sim \mathcal{CN}(0, \sigma_{h_j}^2), \quad v_i, v_j \sim \mathcal{CN}(0, \sigma_v^2).$$

³For non-Gaussian sensing noises, when forming $\tilde{\lambda}_j$, $P(u_i|x_j, \mathcal{H}_\ell)$ and $f(x_j|\mathcal{H}_\ell)$ should be calculated, respectively, based on the joint pdf $f(w_i, w_j)$ and the pdf $f(w_j)$. Also, $P(u_i|x_j, \mathcal{H}_\ell) = P(u_i|\mathcal{H}_\ell)$ when w_i, w_j are mutually independent.

The terms v_i and v_j are the receiver noises at the FC. We assume that noises and fading coefficients are independent and noises are i.i.d. across the pairs. Next, using the signals y_i, y_j and the CSI h_i, h_j for all pairs the FC forms the LRT $\Lambda = \frac{f(y_i, y_j \text{ for all pairs} | \mathcal{H}_1)}{f(y_i, y_j \text{ for all pairs} | \mathcal{H}_0)}$, where $f(y_i, y_j \text{ for all pairs} | \mathcal{H}_\ell)$ indicates the joint pdf of y_i, y_j corresponding to all pairs given the hypothesis \mathcal{H}_ℓ , to make the final decision. We note $\mathcal{H}_\ell \rightarrow \tilde{u}_i, \tilde{u}_j \rightarrow y_i, y_j$ form a Markov chain. Also, (y_i, y_j) are independent across the pairs given \tilde{u}_i, \tilde{u}_j for all pairs. Hence, we can write

$$\begin{aligned} f(y_i, y_j \text{ for all pairs} | \mathcal{H}_\ell) &= \sum_{\tilde{u}_i} \sum_{\tilde{u}_j} f(y_i, y_j \text{ for all pairs} | \tilde{u}_i, \tilde{u}_j \text{ for all pairs}) P(\tilde{u}_i, \tilde{u}_j \text{ for all pairs} | \mathcal{H}_\ell) \\ &= \sum_{\tilde{u}_i} \sum_{\tilde{u}_j} \left(\prod_{\text{for all pairs}} f(y_i, y_j | \tilde{u}_i, \tilde{u}_j \text{ for } (\mathcal{S}_i, \mathcal{S}_j)) \right) P(\tilde{u}_i, \tilde{u}_j \text{ for all pairs} | \mathcal{H}_\ell), \end{aligned} \quad (11)$$

where the sums are taken over all values that \tilde{u}_i, \tilde{u}_j can take. To find $f(y_i, y_j | \tilde{u}_i, \tilde{u}_j \text{ for } (\mathcal{S}_i, \mathcal{S}_j))$ in (11) we realize that in the pair $(\mathcal{S}_i, \mathcal{S}_j)$ given \tilde{u}_i, \tilde{u}_j , the variables y_i and y_j are independent complex Gaussian RVs with the means $\mu_i = \sqrt{\alpha} \tilde{u}_i h_i, \mu_j = \sqrt{\alpha} \tilde{u}_j h_j$ and the variance σ_v^2 . To obtain $P(\tilde{u}_i, \tilde{u}_j \text{ for all pairs} | \mathcal{H}_\ell)$ in (11) we assume that the FC only knows the statistics of inter-node channels g_{ij}, g_{ji} . Note that $\mathcal{H}_\ell \rightarrow x_i, x_j, r_{ij}, r_{ji} \rightarrow \tilde{u}_i, \tilde{u}_j$ forms a Markov chain. Therefore

$$\begin{aligned} P(\tilde{u}_i, \tilde{u}_j \text{ for all pairs} | \mathcal{H}_\ell) &= \\ &\int_{g_{ij}} \int_{g_{ji}} \int_{x_i} \int_{x_j} \int_{r_{ij}} \int_{r_{ji}} P(\tilde{u}_i, \tilde{u}_j \text{ for all pairs} | g_{ij}, g_{ji}, x_i, x_j, r_{ij}, r_{ji} \text{ for all pairs}) \\ &\times f(x_i, x_j, r_{ij}, r_{ji} \text{ for all pairs} | \mathcal{H}_\ell) f(g_{ij}, g_{ji}) dg_{ij} dg_{ji} dx_i dx_j dr_{ij} dr_{ji}. \end{aligned} \quad (12)$$

Equation (12) can be further simplified by noting that given x_i, x_j, r_{ij}, r_{ji} for all pairs, the variables $(\tilde{u}_i, \tilde{u}_j)$ are independent across the pairs. Furthermore, within a pair, given x_i, x_j, r_{ij}, r_{ji} , the variables \tilde{u}_i and \tilde{u}_j are independent. Also, we note that $\mathcal{H}_\ell \rightarrow x_i, x_j \rightarrow r_{ij}, r_{ji}$ forms a Markov chain and given x_i, x_j for all pairs, (r_{ij}, r_{ji}) are independent across the pairs. Besides, within a pair, given x_i, x_j , the variables r_{ij}, r_{ji} are independent. Combining all, we can rewrite (12) as

$$\begin{aligned} &\int_{g_{ij}} \int_{g_{ji}} \int_{x_i} \int_{x_j} \int_{r_{ij}} \int_{r_{ji}} \left(\prod_{\text{for all pairs}} P(\tilde{u}_i | x_i, r_{ji} \text{ for } (\mathcal{S}_i, \mathcal{S}_j)) P(\tilde{u}_j | x_j, r_{ij} \text{ for } (\mathcal{S}_i, \mathcal{S}_j)) \right) \\ &\times f(r_{ji} | x_j \text{ for } (\mathcal{S}_i, \mathcal{S}_j)) f(r_{ij} | x_i \text{ for } (\mathcal{S}_i, \mathcal{S}_j)) f(x_i, x_j \text{ for all pairs} | \mathcal{H}_\ell) f(g_{ij}, g_{ji}) dg_{ij} dg_{ji} dx_i dx_j dr_{ij} dr_{ji}. \end{aligned} \quad (13)$$

Focusing on the term $P(\tilde{u}_i|x_i, r_{ji}$ for $(\mathcal{S}_i, \mathcal{S}_j)$) in (13) we note that $P(\tilde{u}_i = 1|x_i, r_{ji}) = \mathbf{1}_{\{\tilde{\lambda}_i > \pi_0/\pi_1\}}$ and $P(\tilde{u}_i = -1|x_i, r_{ji}) = \mathbf{1}_{\{\tilde{\lambda}_i < \pi_0/\pi_1\}}$ where $\tilde{\lambda}_i$ depends on the inter-node channels g_{ji} , the threshold τ_j , the sensing noise variances $\sigma_{w_i}^2, \sigma_{w_j}^2$ and the correlation coefficient $\rho_{i,j}$. Similarly, we can find $P(\tilde{u}_j|x_j, r_{ij}$ for $(\mathcal{S}_i, \mathcal{S}_j)$) in (13). Considering the term $f(r_{ji}|x_j$ for $(\mathcal{S}_i, \mathcal{S}_j)$) in (13) we find

$$\begin{aligned} f(r_{ji}|x_j \text{ for } (\mathcal{S}_i, \mathcal{S}_j)) &= f(r_{ji}|u_j = 1)P(u_j = 1|x_j) + f(r_{ji}|u_j = -1)P(u_j = -1|x_j) \\ &= f(r_{ji}|u_j = 1)\mathbf{1}_{\{x_j > \tau_j\}} + f(r_{ji}|u_j = -1)\mathbf{1}_{\{x_j < \tau_j\}} \end{aligned} \quad (14)$$

where $f(r_{ji}|u_j)$ in (14) can be found noting that given g_{ji}, u_j we have $r_{ji} \sim \mathcal{CN}(\sqrt{1 - \alpha}u_j g_{ji}, \sigma_\eta^2)$. Considering the term $f(x_i, x_j$ for all pairs $|\mathcal{H}_\ell$) in (13) we note that when Gaussian sensing noises are uncorrelated⁴ we obtain $f(x_i, x_j$ for all pairs $|\mathcal{H}_\ell) = \prod$ for all pairs $f(x_i$ for $(\mathcal{S}_i, \mathcal{S}_j)|\mathcal{H}_\ell) f(x_j$ for $(\mathcal{S}_i, \mathcal{S}_j)|\mathcal{H}_\ell)$. Combining all these one can verify that the probability in (12) depends on sensing channels through $\tau_i, \tau_j, \sigma_{w_i}^2, \sigma_{w_j}^2, \rho_{i,j}$ and the average received SNR $\bar{\gamma}_{hs_{ij}}$ corresponding to $(\mathcal{S}_i, \mathcal{S}_j)$ inter-node communication. When the parameters of sensing channels are unavailable at the FC, the FC demodulates the channel inputs for all pairs using the signals y_i, y_j for all pairs and applies the majority rule to the demodulated symbols to reach the final decision.

V. PARALLEL FUSION ARCHITECTURE WITH LOCAL THRESHOLD CHANGING AT SENSORS

A. Local Decision Rules at Sensors

Suppose nodes \mathcal{S}_i and \mathcal{S}_j are within a pair. Each sensor makes an initial decision based on its measurement. Let u_i denote the decision made at \mathcal{S}_i based on x_i . In the absence of inter-node communication, \mathcal{S}_i assumes that the decision u_j (made at \mathcal{S}_j based on x_j) is different from u_i , i.e., \mathcal{S}_i assumes $u_j = -u_i$. Next, \mathcal{S}_i forms another decision \bar{u}_i by fusing the assumed decision u_j and its measurement x_i . In particular, \mathcal{S}_i forms a local LRT $\bar{\lambda}_i = \frac{f(x_i, u_j = -u_i|\mathcal{H}_1)}{f(x_i, u_j = -u_i|\mathcal{H}_0)}$, where $f(x_i, u_j = -u_i|\mathcal{H}_\ell)$ indicates the joint pdf of x_i and the assumed decision u_j at \mathcal{S}_i given the hypothesis \mathcal{H}_ℓ , to make \bar{u}_i .

⁴For non-Gaussian sensing noises, $\tilde{\lambda}_i$ would change as explained in the previous footnote. Also, $P(u_j|x_j)$ in (14) and $f(x_i, x_j$ for all pairs $|\mathcal{H}_\ell)$ in (13), respectively, should be calculated based on the pdf $f(w_j)$ and the joint pdf $f(w_1, \dots, w_K)$.

Node \mathcal{S}_i lets $\bar{u}_i = 1$ when $\bar{\lambda}_i > \pi_0/\pi_1$ and lets $\bar{u}_i = -1$ otherwise. We find⁵

$$\bar{\lambda}_i = \frac{P(u_j = -u_i|x_i, \mathcal{H}_1)f(x_i|\mathcal{H}_1)}{P(u_j = -u_i|x_i, \mathcal{H}_0)f(x_i|\mathcal{H}_0)}. \quad (15)$$

in which $P(u_j = -u_i|x_i, \mathcal{H}_\ell)$ is given in (10) and $f(x_j|\mathcal{H}_\ell)$ is found by noting⁶ that given \mathcal{H}_ℓ , we have $x_j \sim \mathcal{CN}(\ell, \sigma_{w_j}^2)$. In fact, one can verify that \mathcal{S}_i finds u_i, \bar{u}_i as the following

$$\begin{cases} u_i = 1, \bar{u}_i = 1 & \text{if } x_i > \tau'_{i_1}, & u_i = -1, \bar{u}_i = -1 & \text{if } x_i < \tau'_{i_2} \\ u_i = -1, \bar{u}_i = 1 & \text{if } \tau'_{i_2} < x_i < \tau_i, & u_i = 1, \bar{u}_i = -1 & \text{if } \tau_i < x_i < \tau'_{i_1} \end{cases} \quad (16)$$

where the thresholds τ'_{i_1}, τ'_{i_2} , given in the footnote, depend on $\sigma_{w_i}^2, \rho_{i,j}$ and satisfy $\tau'_{i_2} < \tau_i < \tau'_{i_1}$. When Gaussian sensing noises are uncorrelated the assumed decision u_j and x_i are independent for a given hypothesis \mathcal{H}_ℓ , leading into $P(u_j = -u_i|x_i, \mathcal{H}_\ell) = P(u_j = -u_i|\mathcal{H}_\ell)$ in (15). Consequently, the local LRT $\bar{\lambda}_i$ in (15) can be further simplified and τ'_{i_1}, τ'_{i_2} in (16), respectively, reduce to $\tau_{i_1} = 0.5 + \sigma_{w_i}^2 \ln\left(\frac{(1-P_{f_j})\pi_0}{(1-P_{d_j})\pi_1}\right)$ and $\tau_{i_2} = 0.5 + \sigma_{w_i}^2 \ln\left(\frac{P_{f_j}\pi_0}{P_{d_j}\pi_1}\right)$ where $\tau_{i_2} < \tau_i < \tau_{i_1}$. Since in addition to threshold τ_i employed in scheme (i), x_i is also compared against two additional thresholds τ'_{i_1}, τ'_{i_2} , we refer to scheme (iii) as “local threshold changing”. The pair $(\mathcal{S}_i, \mathcal{S}_j)$ sends $u_i, \bar{u}_i, u_j, \bar{u}_j$ to the FC in two consecutive time slots, exploiting Alamouti’s STC scheme. In particular, in the n th slot, \mathcal{S}_i and \mathcal{S}_j can send simultaneously $\frac{u_i}{\sqrt{2}}$ and $\frac{\bar{u}_j}{\sqrt{2}}$, respectively. In the $(n+1)$ th time slot, \mathcal{S}_i and \mathcal{S}_j can send simultaneously $-\frac{\bar{u}_i}{\sqrt{2}}$ and $\frac{u_j}{\sqrt{2}}$, respectively. Considering the definitions of channel variances, we note that effectively \mathcal{S}_i spends $\mathcal{P} = \frac{1}{2}\mathcal{P} + \frac{1}{2}\mathcal{P}$ for sensor-FC communication.

B. Node-FC Communication Channel Model and Fusion Rule at FC

Let $y_{ij}(n)$ and $y_{ij}(n+1)$ denote the received signals at the FC corresponding to the pair $(\mathcal{S}_i, \mathcal{S}_j)$ during two consecutive time slots. The signal model in (5) still holds true, after substituting $\sqrt{\frac{\alpha}{2}}$ with

⁵Consider a hypothetical case where \mathcal{S}_i assumes $u_j = -1$ and makes a decision u_i^0 by optimally fusing the assumed $u_j = -1$ and x_i . In particular, \mathcal{S}_i lets $u_i^0 = 1$ when $\lambda_i^0 = \frac{f(x_i, u_j = -1|\mathcal{H}_1)}{f(x_i, u_j = -1|\mathcal{H}_0)} > \frac{\pi_0}{\pi_1}$ and lets $u_i^0 = -1$ otherwise. Consider another hypothetical case where \mathcal{S}_i assumes $u_j = 1$ and makes a decision u_i^1 by optimally fusing the assumed $u_j = 1$ and x_i . In particular, \mathcal{S}_i lets $u_i^1 = 1$ when $\lambda_i^1 = \frac{f(x_i, u_j = 1|\mathcal{H}_1)}{f(x_i, u_j = 1|\mathcal{H}_0)} > \frac{\pi_0}{\pi_1}$ and lets $u_i^1 = -1$ otherwise. One can verify $u_i^0 = 1$ when $x_i > \tau'_{i_1}$ and $u_i^0 = -1$ otherwise, also $u_i^1 = 1$ when $x_i > \tau'_{i_2}$ and $u_i^1 = -1$ otherwise, where $\tau'_{i_1} = 0.5 + \sigma_{w_i}^2 \ln\left(\frac{P(u_j = -1|x_i, \mathcal{H}_0)\pi_0}{P(u_j = -1|x_i, \mathcal{H}_1)\pi_1}\right)$ and $\tau'_{i_2} = 0.5 + \sigma_{w_i}^2 \ln\left(\frac{P(u_j = 1|x_i, \mathcal{H}_0)\pi_0}{P(u_j = 1|x_i, \mathcal{H}_1)\pi_1}\right)$ and $\tau'_{i_2} < \tau_i < \tau'_{i_1}$. For these hypothetical cases, now suppose $x_i < \tau_i$ and thus $u_i = -1$. Since $\tau_i < \tau'_{i_1}$ we have $x_i < \tau'_{i_1}$ and thus $u_i^0 = -1$, i.e., $u_i^0 = u_i$, whereas u_i^1 can be ± 1 . Therefore, the useful information is embedded in u_i, u_i^1 , as u_i^0 does not convey extra information. Similarly, one can argue that when $x_i > \tau_i$ the useful information is imbedded in u_i, u_i^0 , as u_i^1 does not convey extra information. In conclusion, node \mathcal{S}_i should assume $u_j = -u_i$ to be able to extract more information from x_i .

⁶For non-Gaussian sensing noises, similar to $\bar{\lambda}_i$ in Section IV-A, $\bar{\lambda}_i$ would change. In particular, $P(u_j|x_i, \mathcal{H}_\ell)$ and $f(x_i|\mathcal{H}_\ell)$ should be calculated, respectively, based on the joint pdf $f(w_i, w_j)$ and the pdf $f(w_i)$.

$\frac{1}{\sqrt{2}}$, u_j with \bar{u}_j , \hat{u}_j with \bar{u}_i , and \hat{u}_i with u_j . We can take similar steps as in Section III-B to find the signals z_i, z_j using $y_{ij}(n), y_{ij}^*(n+1)$. Next, using the signals z_i, z_j and the CSI h_i, h_j for all pairs the FC forms the LRT $\Lambda = \frac{f(z_i, z_j \text{ for all pairs} | \mathcal{H}_1)}{f(z_i, z_j \text{ for all pairs} | \mathcal{H}_0)}$. We note $\mathcal{H}_\ell \rightarrow u_i, u_j, \bar{u}_i, \bar{u}_j \rightarrow z_i, z_j$ forms a Markov chain. Also, (z_i, z_j) are independent across the pairs given $u_i, u_j, \bar{u}_i, \bar{u}_j$ for all pairs. Therefore

$$f(z_i, z_j \text{ for all pairs} | \mathcal{H}_\ell) = \sum_{u_i \text{ for all pairs}} \sum_{u_j \text{ for all pairs}} \sum_{\bar{u}_i \text{ for all pairs}} \sum_{\bar{u}_j \text{ for all pairs}} \left(\prod_{\text{for all pairs}} f(z_i, z_j | u_i, u_j, \bar{u}_i, \bar{u}_j \text{ for } (\mathcal{S}_i, \mathcal{S}_j)) \right) P(u_i, u_j, \bar{u}_i, \bar{u}_j \text{ for all pairs} | \mathcal{H}_\ell). \quad (17)$$

Focusing on the term $f(z_i, z_j | u_i, u_j, \bar{u}_i, \bar{u}_j \text{ for } (\mathcal{S}_i, \mathcal{S}_j))$ in (17) we realize that z_i, z_j are conditionally independent complex Gaussian RVs with the variance $\sigma^2 = (|h_i|^2 + |h_j|^2)\sigma_v^2$ and the means μ_i, μ_j given in (7), after substituting $\sqrt{\frac{\alpha}{2}}$ with $\frac{1}{\sqrt{2}}$, u_j with \bar{u}_j , \hat{u}_j with \bar{u}_i , and \hat{u}_i with u_j . To find $P(u_i, u_j, \bar{u}_i, \bar{u}_j \text{ for all pairs} | \mathcal{H}_\ell)$ we note this term can be expressed in terms of the probability of x_i, x_j being in certain intervals for all pairs. For instance, $P(u_i = \bar{u}_i = 1, u_j = \bar{u}_j = -1 \text{ for all pairs} | \mathcal{H}_\ell) = P(x_i > \tau_{ij_1}, x_j < \tau_{ij_2} \text{ for all pairs} | \mathcal{H}_\ell)$. Now, these probabilities can be easily characterized for the sensing channel model in Section II-A, where x_i, x_j are jointly correlated Gaussian RVs with known statistics⁷. When Gaussian sensing noises are uncorrelated the decisions (u_i, \bar{u}_i) and (u_j, \bar{u}_j) given hypothesis \mathcal{H}_ℓ are independent across the pairs. Therefore $P(u_i, u_j, \bar{u}_i, \bar{u}_j \text{ for all pairs} | \mathcal{H}_\ell) = \prod_{\text{for all pairs}} P(u_i, \bar{u}_i \text{ for } (\mathcal{S}_i, \mathcal{S}_j) | \mathcal{H}_\ell) P(u_j, \bar{u}_j \text{ for } (\mathcal{S}_i, \mathcal{S}_j) | \mathcal{H}_\ell)$. When the parameters of sensing channels are unavailable at the FC, the FC demodulates the channel inputs for all pairs using the signals z_i, z_j for all pairs and applies the majority rule to the demodulated symbols to reach the final decision.

VI. PERFORMANCE ANALYSIS

Section VI-A provides an upper bound on the average error probability for scheme (i) of Section III. Leveraging on this, sections VI-B and VI-C, respectively, provide upper bounds on the average error probability for the classical parallel fusion architecture of Section II-B and scheme (ii) of Section IV. For mathematical tractability, we assume that the Gaussian sensing noises w_k are identically distributed and uncorrelated⁸, i.e., we have $\sigma_{w_k}^2 = \sigma_w^2, \tau_k = \tau$ and thus $P_{d_k} = P_d, P_{f_k} = P_f$. Also, we assume that sensors are positioned equally distant from the FC and thus $\bar{\gamma}_h^2 = \frac{\sigma_w^2}{\sigma_v^2}$. Also, distances between the cooperative

⁷For non-Gaussian w_k 's, $P(u_i, u_j, \bar{u}_i, \bar{u}_j \text{ for all pairs} | \mathcal{H}_\ell)$ should be calculated in terms of the joint pdf $f(w_1, \dots, w_K)$.

⁸The derivations in this section also hold true for i.i.d sensing noises.

partners are assumed equal across the pairs and therefore $\bar{\gamma}_{h_s}^2 = \frac{(1-\alpha)\sigma_{h_s}^2}{\sigma_\eta^2}$. In Section VII we validate the analytical results of this section via Monte-Carlo simulations.

A. Cooperative Fusion Architecture with STC at Sensors

For performance analysis, suppose each pair of cooperative partners $(\mathcal{S}_i, \mathcal{S}_j)$ is associated with a unique group index s where $s = 1, \dots, S$ and $S = K/2$. We denote the two nodes within the group s as $(\mathcal{S}_{2s-1}, \mathcal{S}_{2s})$, i.e., we map the indices i, j in Section III into $2s-1, 2s$, respectively. For LRT fusion rule in Section III-B, the conditional error probability is $P_{e|h} = P_{e_1|h} + P_{e_2|h}$ where $P_{e_1|h} = P(\Lambda > \frac{\pi_0}{\pi_1} | \mathcal{H}_0) \pi_0$ and $P_{e_2|h} = P(\Lambda < \frac{\pi_0}{\pi_1} | \mathcal{H}_1) \pi_1$ and $\Lambda = \frac{f(z_{2s-1}, z_{2s} \text{ for } s=1, \dots, S | \mathcal{H}_1)}{f(z_{2s-1}, z_{2s} \text{ for } s=1, \dots, S | \mathcal{H}_0)}$, conditioned on the channel coefficients h_{2s-1}, h_{2s} for $s = 1, \dots, S$ at the FC. The average error probability $\bar{P}_e = \bar{P}_{e_1} + \bar{P}_{e_2}$ is obtained by taking the averages of $P_{e_1|h}, P_{e_2|h}$ over the distribution of the channel coefficients. Our goal is to provide upper bounds on $P_{e_1|h}, P_{e_2|h}$ and their corresponding averages $\bar{P}_{e_1} = \mathbb{E}\{P_{e_1|h}\}, \bar{P}_{e_2} = \mathbb{E}\{P_{e_2|h}\}$. We use the following notation in our derivations. To capture all different values that $u_{2s-1}, u_{2s}, \hat{u}_{2s-1}, \hat{u}_{2s}$ for $s = 1, \dots, S$ can take we consider two K -length sequences $(a_{n_1}^1, a_{n_1}^2, \dots, a_{n_1}^{2s-1}, a_{n_1}^{2s}, \dots, a_{n_1}^{2S-1}, a_{n_1}^{2S})$ and $(a_{m_1}^1, a_{m_1}^2, \dots, a_{m_1}^{2s-1}, a_{m_1}^{2s}, \dots, a_{m_1}^{2S-1}, a_{m_1}^{2S})$ where $a_{n_1}^{2s-1}, a_{n_1}^{2s} \in \{1, -1\}$ are the values assumed by u_{2s-1}, u_{2s} and $a_{m_1}^{2s-1}, a_{m_1}^{2s} \in \{1, -1\}$ are the values assumed by $\hat{u}_{2s-1}, \hat{u}_{2s}$. Also, let n_1 and m_1 , respectively, be the decimal numbers corresponding to the two K -length binary sequences, when those $a_{n_1}^k$ and $a_{m_1}^k$ assuming -1 value in the sequences are reassigned 0 value. Let Q_{n_1} denote the number of ones in the sequence $(a_{n_1}^1, a_{n_1}^2, \dots, a_{n_1}^{2s-1}, a_{n_1}^{2s}, \dots, a_{n_1}^{2S-1}, a_{n_1}^{2S})$. Define $F_{n_1, m_1}, F_{n_1}, T_{n_1, m_1}, d_{n_1, m_1}$ as below

$$F_{n_1, m_1} = \{u_{2s-1} = a_{n_1}^{2s-1}, u_{2s} = a_{n_1}^{2s}, \hat{u}_{2s-1} = a_{m_1}^{2s-1}, \hat{u}_{2s} = a_{m_1}^{2s} \text{ for } s=1, \dots, S\} \quad (18)$$

$$F_{n_1} = \{u_{2s-1} = a_{n_1}^{2s-1}, u_{2s} = a_{n_1}^{2s} \text{ for } s=1, \dots, S\} \quad (19)$$

$$T_{n_1, m_1} = \prod_{s=1}^S P(\hat{u}_{2s-1} = a_{m_1}^{2s-1} | u_{2s-1} = a_{n_1}^{2s-1}) P(\hat{u}_{2s} = a_{m_1}^{2s} | u_{2s} = a_{n_1}^{2s}) \quad (20)$$

$$d_{n_1, m_1} = (\pi_1 P_d^{Q_{n_1}} (1 - P_d)^{K-Q_{n_1}} - \pi_0 P_f^{Q_{n_1}} (1 - P_f)^{K-Q_{n_1}}) T_{n_1, m_1} \\ \times \prod_{s=1}^S f(z_{2s-1}, z_{2s} | u_{2s-1} = a_{n_1}^{2s-1}, u_{2s} = a_{n_1}^{2s}, \hat{u}_{2s-1} = a_{m_1}^{2s-1}, \hat{u}_{2s} = a_{m_1}^{2s}). \quad (21)$$

Furthermore, let M be an integer that satisfies $\frac{P_d^M (1-P_d)^{K-M}}{P_f^M (1-P_f)^{K-M}} > \frac{\pi_0}{\pi_1}$ and $\frac{P_d^{M-1} (1-P_d)^{K-M+1}}{P_f^{M-1} (1-P_f)^{K-M+1}} < \frac{\pi_0}{\pi_1}$, i.e., M is the smallest number of nodes that can decide \mathcal{H}_1 while \mathcal{H}_1 is true and the FC decides correctly, had all communication channels were error-free. Define the sets $S_0 = \{d_{n_1, m_1} \text{ where } Q_{n_1} < M\}$ and $S_1 = \{d_{n_1, m_1} \text{ where } Q_{n_1} \geq M\}$. Note that all entries of S_0 and S_1 are, respectively, negative and positive.

Let $|S_0|$ and $|S_1|$ denote the cardinalities of S_0 and S_1 , respectively. Utilizing the above notations, we can rewrite $f(z_{2s-1}, z_{2s})$ for $s = 1, \dots, S|\mathcal{H}_\ell$ in Λ as

$$f(z_{2s-1}, z_{2s} \text{ for } s = 1, \dots, S|\mathcal{H}_\ell) = \sum_{n_1, m_1} P(F_{n_1}|\mathcal{H}_\ell) T_{n_1, m_1} \quad (22)$$

$$\times \prod_{s=1}^S f(z_{2s-1}, z_{2s} | u_{2s-1} = a_{n_1}^{2s-1}, u_{2s} = a_{n_1}^{2s}, \hat{u}_{2s-1} = a_{m_1}^{2s-1}, \hat{u}_{2s} = a_{m_1}^{2s}).$$

Since sensing noises are identically distributed and uncorrelated we find $P(F_{n_1}|\mathcal{H}_\ell) = \prod_{s=1}^S P(u_{2s-1} = a_{n_1}^{2s-1}|\mathcal{H}_\ell)P(u_{2s} = a_{n_1}^{2s}|\mathcal{H}_\ell)$ in (22), and thus $P(F_{n_1}|\mathcal{H}_1) = P_d^{Q_{n_1}}(1 - P_d)^{K-Q_{n_1}}$ and $P(F_{n_1}|\mathcal{H}_0) = P_f^{Q_{n_1}}(1 - P_f)^{K-Q_{n_1}}$. The term T_{n_1, m_1} in (22) is calculated using (8) and depends on the average received SNR $\bar{\gamma}_{hs}$ corresponding to inter-node communication. Combining (21), (22) we have

$$P_{e_1|h} = \pi_0 P\left(\sum_{n_1, m_1} d_{n_1, m_1} > 0 | \mathcal{H}_0\right) = \pi_0 \sum_{n, m} \mathcal{T}_{e_1|h} P(F_{n, m}|\mathcal{H}_0) = \pi_0 \sum_{n, m} \mathcal{T}_{e_1|h} P_f^{Q_n} (1 - P_f)^{K-Q_n} T_{n, m} \quad (23)$$

$$P_{e_2|h} = \pi_1 P\left(\sum_{n_1, m_1} d_{n_1, m_1} < 0 | \mathcal{H}_1\right) = \pi_1 \sum_{n, m} \mathcal{T}_{e_2|h} P(F_{n, m}|\mathcal{H}_1) = \pi_1 \sum_{n, m} \mathcal{T}_{e_2|h} P_d^{Q_n} (1 - P_d)^{K-Q_n} T_{n, m}. \quad (24)$$

where $\mathcal{T}_{e_1|h} = P(\sum_{n_1, m_1} d_{n_1, m_1} > 0 | F_{n, m})$ in (23) and $\mathcal{T}_{e_2|h} = 1 - \mathcal{T}_{e_1|h}$ in (24). Note that $P_{e_1|h}$ in (23) and $P_{e_2|h}$ in (24) depend on h_{2s-1}, h_{2s} for $s = 1, \dots, S$ only through $\mathcal{T}_{e_1|h}$ and $\mathcal{T}_{e_2|h}$, respectively. These imply that the problem of finding upper bounds on $P_{e_1|h}, P_{e_2|h}$ and their corresponding averages $\bar{P}_{e_1}, \bar{P}_{e_2}$ can be reduced to finding upper bounds on $\mathcal{T}_{e_1|h}, \mathcal{T}_{e_2|h}$ and their respective averages $\bar{\mathcal{T}}_{e_1} = \mathbb{E}\{\mathcal{T}_{e_1|h}\}, \bar{\mathcal{T}}_{e_2} =$

$\mathbb{E}\{\mathcal{T}_{e_2|h}\}$. In Appendix A we establish the following

$$\bar{\mathcal{T}}_{e_1} < \frac{\mathbf{1}_{\{Q_n < M\}}}{2\sqrt{|S_1|}} \sum_{d_{n_1, m_1} \in S_1} [\sqrt{G(n, m, n_1, m_1)} \prod_{s=1}^S \mathcal{D}_1(n, m, n_1, m_1)] + \mathbf{1}_{\{Q_n \geq M\}}, \quad (25)$$

$$\bar{\mathcal{T}}_{e_2} < \frac{\mathbf{1}_{\{Q_n > M\}}}{|S_0|} \sum_{d_{n_1, m_1} \in S_0} [\min_t (|S_0|G(n, m, n_1, m_1))^t \prod_{s=1}^S \mathcal{D}_2(n, m, n_1, m_1)] + \mathbf{1}_{\{Q_n \leq M\}}, \quad (26)$$

$$G(n, m, n_1, m_1) = \frac{(\pi_1 P_d^{Q_{n_1}} (1 - P_d)^{K - Q_{n_1}} - \pi_0 P_f^{Q_{n_1}} (1 - P_f)^{K - Q_{n_1}})}{(\pi_0 P_f^{Q_n} (1 - P_f)^{K - Q_n} - \pi_1 P_d^{Q_n} (1 - P_d)^{K - Q_n})} \times \frac{T_{n_1, m_1}}{T_{n, m}}, \quad (27)$$

$$\mathcal{D}_1(n, m, n_1, m_1) = \left(\left(1 + \frac{\alpha \bar{\gamma}_h \bar{a}_1}{8}\right) \left(1 + \frac{\alpha \bar{\gamma}_h \bar{a}_2}{8}\right) - \frac{\alpha^2 \bar{\gamma}_h^2 \bar{a}_3}{64} \right)^{-1}, \quad (28)$$

$$\mathcal{D}_2(n, m, n_1, m_1) = \left(\left(1 + \frac{\alpha(t^2 - t) \bar{\gamma}_h \bar{a}_1}{2}\right) \left(1 + \frac{\alpha(t^2 - t) \bar{\gamma}_h \bar{a}_2}{2}\right) - \frac{\alpha^2(t^2 - t)^2 \bar{\gamma}_h^2 \bar{a}_3}{16} \right)^{-1}, \quad (29)$$

$$\bar{a}_1 = (a_n^{2s-1} - a_{n_1}^{2s-1})^2 + (a_n^{2s} - a_{n_1}^{2s})^2, \quad \bar{a}_2 = (a_m^{2s-1} - a_{m_1}^{2s-1})^2 + (a_m^{2s} - a_{m_1}^{2s})^2,$$

$$\bar{a}_3 = (a_n^{2s-1} - a_{n_1}^{2s-1})(a_n^{2s} - a_{n_1}^{2s}) - (a_m^{2s-1} - a_{m_1}^{2s-1})(a_m^{2s} - a_{m_1}^{2s}).$$

The upper bound on $\bar{\mathcal{T}}_{e_2}$ depends on t . Our simulations indicate that the bound is minimized for $t \approx 0.3$. Furthermore, the upper bounds depend on the power allocation parameter α . In Section VII we investigate the optimal α that minimizes these bounds. In the ideal case when the inter-node communication is error-free we find $a_n^{2s-1} = a_m^{2s-1}$ and $a_n^{2s} = a_m^{2s}$ and thus (28) and (29), respectively, reduce to $\mathcal{D}_1(n, m, n_1, m_1) = (1 + \frac{\alpha \bar{\gamma}_h \bar{a}_1}{8})^{-2}$, $\mathcal{D}_2(n, m, n_1, m_1) = (1 + \frac{\alpha(t^2 - t) \bar{\gamma}_h \bar{a}_1}{2})^{-2}$.

B. Classical Parallel Fusion Architecture

Leveraging on the derivations in Section VI-A, we provide upper bounds on $\bar{\mathcal{T}}_{e_1}, \bar{\mathcal{T}}_{e_2}$. In fact, the absence of inter-node communication renders the notations in Section VI-A simple, as the indices m, m_1 and the decisions $\hat{u}_{2s-1}, \hat{u}_{2s}$ are dropped, z_{2s-1}, z_{2s} are substituted with y_{2s-1}, y_{2s} and the noises δ_s^1, δ_s^2 are substituted with v_{2s-1}, v_{2s} . Consequently the derivations of the upper bounds become rather easy. In particular, instead of d_{n_1, m_1} in (21), we define d_{n_1} as the following

$$d_{n_1} = (\pi_1 P_d^{Q_{n_1}} (1 - P_d)^{K - Q_{n_1}} - \pi_0 P_f^{Q_{n_1}} (1 - P_f)^{K - Q_{n_1}}) \prod_{s=1}^S f(y_{2s-1}, y_{2s} | u_{2s-1} = a_{n_1}^{2s-1}, u_{2s} = a_{n_1}^{2s}). \quad (30)$$

Also, the relationship between $P_{e_1|h}, \mathcal{T}_{e_1|h}$ in (23) and $P_{e_2|h}, \mathcal{T}_{e_2|h}$ in (24) can be revised as the following

$$\begin{aligned} P_{e_1|h} &= \pi_0 P\left(\sum_{n_1} d_{n_1} > 0 | \mathcal{H}_0\right) = \pi_0 \sum_n \mathcal{T}_{e_1|h} P(F_n | \mathcal{H}_0), \\ P_{e_2|h} &= \pi_1 P\left(\sum_{n_1} d_{n_1} < 0 | \mathcal{H}_1\right) = \pi_1 \sum_n \mathcal{T}_{e_2|h} P(F_n | \mathcal{H}_1). \end{aligned} \quad (31)$$

in which F_n is defined in (19). We redefine $S_0 = \{d_{n_1} \text{ where } Q_{n_1} < M\}$ and $S_1 = \{d_{n_1} \text{ where } Q_{n_1} \geq M\}$, where all entries of S_0 and S_1 are, respectively, negative and positive. We have

$$\begin{aligned} \mathcal{T}_{e_1|h} &< \frac{1}{|S_1|} \sum_{d_{n_1} \in S_1} P(|S_1| d_{n_1} > -d_n | F_n) = \frac{1}{|S_1|} \sum_{d_{n_1} \in S_1} P\left(\zeta(n, n_1) > -\ln(|S_1| G(n, n_1)) + I(n, n_1)\right), \\ \mathcal{T}_{e_2|h} &< \frac{1}{|S_0|} \sum_{d_{n_1} \in S_0} P(d_n < -|S_0| d_{n_1} | F_n) = \frac{1}{|S_0|} \sum_{d_{n_1} \in S_0} P\left(\zeta(n, n_1) > -\ln(|S_0| G(n, n_1)) + I(n, n_1)\right), \\ G(n, n_1) &= \frac{\pi_1 P_d^{Q_{n_1}} (1 - P_d)^{K - Q_{n_1}} - \pi_0 P_f^{Q_{n_1}} (1 - P_f)^{K - Q_{n_1}}}{\pi_0 P_f^{Q_n} (1 - P_f)^{K - Q_n} - \pi_1 P_d^{Q_n} (1 - P_d)^{K - Q_n}}, \\ I(n, n_1) &= \sum_{s=1}^S \mathcal{K}_s(n, n_1) \text{ where } \mathcal{K}_s(n, n_1) = \frac{1}{\sigma_v^2} (|h_{2s-1}(a_{n_1}^{2s-1} - a_n^{2s-1})|^2 + |h_{2s}(a_{n_1}^{2s} - a_n^{2s})|^2), \\ \zeta(n, n_1) &= \sum_{s=1}^S \theta_s(n, n_1) \text{ where } \theta_s(n, n_1) = \frac{2}{\sigma_v} \Re\{v_{2s-1} h_{2s-1}(a_{n_1}^{2s-1} - a_n^{2s-1}) + v_{2s} h_{2s}(a_{n_1}^{2s} - a_n^{2s})\}. \end{aligned}$$

Note that $\zeta(n, n_1)$ is a zero mean Gaussian RV with the variance $2I(n, n_1)$. Using similar techniques in Section VI-A we can establish the following

$$\bar{\mathcal{T}}_{e_1} < \frac{\mathbf{1}_{\{Q_n < M\}}}{2\sqrt{|S_1|}} \sum_{d_{n_1} \in S_1} [\sqrt{G(n, n_1)} \prod_{s=1}^S \mathcal{D}_1(n, n_1)] + \mathbf{1}_{\{Q_n \geq M\}}, \quad (32)$$

$$\bar{\mathcal{T}}_{e_2} < \frac{\mathbf{1}_{\{Q_n > M\}}}{|S_0|} \sum_{d_{n_1} \in S_0} [\min_t (|S_0| G(n, n_1))^t \prod_{s=1}^S \mathcal{D}_2(n, n_1)] + \mathbf{1}_{\{Q_n \leq M\}}, \quad (33)$$

$$\mathcal{D}_1(n, n_1) = \left(\left(1 + \frac{\bar{\gamma} h |a_n^{2s-1} - a_{n_1}^{2s-1}|}{2}\right) \left(1 + \frac{\bar{\gamma} h |a_n^{2s} - a_{n_1}^{2s}|}{2}\right) \right)^{-1}, \quad (34)$$

$$\mathcal{D}_2(n, n_1) = \left(\left(1 + \frac{4(t^2 - t)\bar{\gamma} h |a_n^{2s-1} - a_{n_1}^{2s-1}|}{2}\right) \left(1 + \frac{4(t^2 - t)\bar{\gamma} h |a_n^{2s} - a_{n_1}^{2s}|}{2}\right) \right)^{-1}. \quad (35)$$

This completes our derivations for the upper bounds on $\bar{\mathcal{T}}_{e_1}, \bar{\mathcal{T}}_{e_2}$ and thus $\bar{P}_{e_1}, \bar{P}_{e_2}$. Our simulations indicate that the bound is minimized for $t \approx 0.3$.

C. Cooperative Fusion Architecture with Signal Fusion at Sensors

Leveraging on the derivations in Sections VI-A and VI-B, we provide upper bounds on $\bar{\mathcal{T}}_{e_1}, \bar{\mathcal{T}}_{e_2}$. In fact, the absence of inter-node communication renders the notations in Section VI-A simple, as the indices m, m_1 and the decisions $\hat{u}_{2s-1}, \hat{u}_{2s}$ are dropped, z_{2s-1}, z_{2s} are substituted with y_{2s-1}, y_{2s} and the noises δ_s^1, δ_s^2 are substituted with v_{2s-1}, v_{2s} . Thus the derivations of the upper bounds become rather easy. In particular, instead of d_{n_1, m_1} in (21) or d_{n_1} in (30), we define d_{n_1} as the following

$$\begin{aligned} d_{n_1} &= (\pi_1 \prod_{s=1}^S P(\tilde{u}_{2s-1} = a_{n_1}^{2s-1}, \tilde{u}_{2s} = a_{n_1}^{2s} | \mathcal{H}_1) - \pi_0 \prod_{s=1}^S P(\tilde{u}_{2s-1} = a_{n_1}^{2s-1}, \tilde{u}_{2s} = a_{n_1}^{2s} | \mathcal{H}_0)) \\ &\times \prod_{s=1}^S f(y_{2s-1}, y_{2s} | \tilde{u}_{2s-1} = a_{n_1}^{2s-1}, \tilde{u}_{2s} = a_{n_1}^{2s}). \end{aligned} \quad (36)$$

where $P(\tilde{u}_{2s-1} = a_{n_1}^{2s-1}, \tilde{u}_{2s} = a_{n_1}^{2s} | \mathcal{H}_\ell)$ in (36) is determined in Section IV-B. In fact, this probability depends on sensing channels through the threshold τ and the sensing noise variance σ_w^2 as well as the average received SNR $\bar{\gamma}_{hs}$ corresponding to inter-node communication. Furthermore, the relationship between $P_{e_1|h}, \mathcal{T}_{e_1|h}$ in (23) and $P_{e_2|h}, \mathcal{T}_{e_2|h}$ in (24) can be revised as (31), in which $F_n = \{\tilde{u}_{2s-1} = a_n^{2s-1}, \tilde{u}_{2s} = a_n^{2s} \text{ for } s = 1, \dots, S\}$. We also redefine $S_0 = \{d_{n_1} \text{ where } d_{n_1} < 0\}$ and $S_1 = \{d_{n_1} \text{ where } d_{n_1} \geq 0\}$, where all entries of S_0 and S_1 are, respectively, negative and positive. We have

$$\begin{aligned} \mathcal{T}_{e_1|h} &< \frac{1}{|S_1|} \sum_{d_{n_1} \in S_1} P(|S_1| d_{n_1} > -d_n | F_n) = \frac{1}{|S_1|} \sum_{d_{n_1} \in S_1} P\left(\zeta(n, n_1) > -\ln(|S_1| G(n, n_1)) + I(n, n_1)\right), \\ \mathcal{T}_{e_2|h} &< \frac{1}{|S_0|} \sum_{d_{n_1} \in S_0} P(d_n < -|S_0| d_{n_1} | F_n) = \frac{1}{|S_0|} \sum_{d_{n_1} \in S_0} P\left(\zeta(n, n_1) > -\ln(|S_0| G(n, n_1)) + I(n, n_1)\right), \end{aligned}$$

in which $G(n, n_1) = \frac{(\pi_1 \prod_{s=1}^S P(\tilde{u}_{2s-1} = a_{n_1}^{2s-1}, \tilde{u}_{2s} = a_{n_1}^{2s} | \mathcal{H}_1) - \pi_0 \prod_{s=1}^S P(\tilde{u}_{2s-1} = a_{n_1}^{2s-1}, \tilde{u}_{2s} = a_{n_1}^{2s} | \mathcal{H}_0))}{(\pi_0 \prod_{s=1}^S P(\tilde{u}_{2s-1} = a_{n_1}^{2s-1}, \tilde{u}_{2s} = a_{n_1}^{2s} | \mathcal{H}_0) - \pi_1 \prod_{s=1}^S P(\tilde{u}_{2s-1} = a_{n_1}^{2s-1}, \tilde{u}_{2s} = a_{n_1}^{2s} | \mathcal{H}_1))}$,

$$\begin{aligned} I(n, n_1) &= \sum_{s=1}^S \mathcal{K}_s(n, n_1) \text{ where } \mathcal{K}_s(n, n_1) = \frac{\alpha}{\sigma_v^2} (|h_{2s-1}(a_{n_1}^{2s-1} - a_n^{2s-1})|^2 + |h_{2s}(a_{n_1}^{2s} - a_n^{2s})|^2), \\ \zeta(n, n_1) &= \sum_{s=1}^S \theta_s(n, n_1) \text{ where } \theta_s(n, n_1) = \frac{2\sqrt{\alpha}}{\sigma_v^2} \Re\{v_{2s-1} h_{2s-1}(a_{n_1}^{2s-1} - a_n^{2s-1}) + v_{2s} h_{2s}(a_{n_1}^{2s} - a_n^{2s})\}. \end{aligned}$$

Note that $\zeta(n, n_1)$ is a zero mean Gaussian RV with the variance $2I(n, n_1)$. Using similar techniques in Sections VI-A and VI-B we can establish the following

$$\bar{\mathcal{T}}_{e_1} < \frac{\mathbf{1}_{\{d_n \in S_0\}}}{2\sqrt{|S_1|}} \sum_{d_{n_1} \in S_1} [\sqrt{G(n, n_1)} \prod_{s=1}^S \mathcal{D}_1(n, n_1)] + \mathbf{1}_{\{d_n \in S_1\}}, \quad (37)$$

$$\bar{\mathcal{T}}_{e_2} < \frac{\mathbf{1}_{\{d_n \in S_1\}}}{|S_0|} \sum_{d_{n_1} \in S_1} [\min_t (|S_0|G(n, n_1))^t \prod_{s=1}^S \mathcal{D}_2(n, n_1)] + \mathbf{1}_{\{d_n \in S_0\}}, \quad (38)$$

$$\mathcal{D}_1(n, n_1) = \left(\left(1 + \frac{\alpha \bar{\gamma}_h (a_n^{2s-1} - a_{n_1}^{2s-1})^2}{4}\right) \left(1 + \frac{\alpha \bar{\gamma}_h (a_n^{2s} - a_{n_1}^{2s})^2}{4}\right) \right)^{-1}, \quad (39)$$

$$\mathcal{D}_2(n, n_1) = ((1 + \alpha(t^2 - t)\bar{\gamma}_h(a_n^{2s-1} - a_{n_1}^{2s-1})^2)(1 + \alpha(t^2 - t)\bar{\gamma}_h(a_n^{2s} - a_{n_1}^{2s})^2))^{-1}. \quad (40)$$

This completes our derivations for the upper bounds on $\bar{\mathcal{T}}_{e_1}, \bar{\mathcal{T}}_{e_2}$ and thus $\bar{P}_{e_1}, \bar{P}_{e_2}$. Our numerical results show that the bound is minimized for $t \approx 0.3$. Furthermore, the upper bounds depend on the power allocation parameter α . In Section VII we investigate the optimal α that minimizes these bounds.

D. Parallel Fusion Architecture with Local Threshold Changing at Sensors

Leveraging on the derivations in sections VI-A and VI-B, we provide upper bounds on $\bar{\mathcal{T}}_{e_1}, \bar{\mathcal{T}}_{e_2}$. To capture all different values that $u_{2s-1}, u_{2s}, \bar{u}_{2s-1}, \bar{u}_{2s}$ for $s = 1, \dots, S$ can take we consider a $2K$ -length sequence $(a_{n_1}^1, a_{n_1}^2, a_{m_1}^1, a_{m_1}^2, \dots, a_{n_1}^{2S-1}, a_{n_1}^{2S}, a_{m_1}^{2S-1}, a_{m_1}^{2S})$ where $a_{n_1}^{2s-1}, a_{n_1}^{2s} \in \{1, -1\}$ and $a_{m_1}^{2s-1}, a_{m_1}^{2s} \in \{1, -1\}$, respectively, are the values assumed by u_{2s-1}, u_{2s} and $\bar{u}_{2s-1}, \bar{u}_{2s}$. Let $Q_{n_1, m_1}^1, Q_{n_1, m_1}^2, Q_{n_1, m_1}^3, Q_{n_1, m_1}^4$, respectively, denote the number of cases in the above sequence that $a_{n_1}^{s'} = a_{m_1}^{s'} = 1$, $a_{n_1}^{s'} = -a_{m_1}^{s'} = 1$, $a_{n_1}^{s'} = -a_{m_1}^{s'} = -1$, and $a_{n_1}^{s'} = a_{m_1}^{s'} = -1$ for $s' = 2s, 2s-1, s = 1, \dots, S$. Instead of F_{n_1, m_1} in (17) and d_{n_1, m_1} in (18), we redefine them as the following

$$\begin{aligned} F_{n_1, m_1} &= \{u_{2s-1} = a_{n_1}^{2s-1}, u_{2s} = a_{n_1}^{2s}, \bar{u}_{2s-1} = a_{m_1}^{2s-1}, \bar{u}_{2s} = a_{m_1}^{2s} \text{ for } s=1, \dots, S\}, \\ d_{n_1, m_1} &= (\pi_1 \prod_{j=1}^4 P_{d_j}^{Q_{n_1, m_1}^j} - \pi_0 \prod_{j=1}^4 P_{f_j}^{Q_{n_1, m_1}^j}) \\ &\quad \times \prod_{s=1}^S f(z_{2s-1}, z_{2s} | u_{2s-1} = a_{n_1}^{2s-1}, u_{2s} = a_{n_1}^{2s}, \bar{u}_{2s-1} = a_{m_1}^{2s-1}, \bar{u}_{2s} = a_{m_1}^{2s}), \end{aligned} \quad (41)$$

where $P(\bar{u}_i = 1 | u_i = -u_j = -1, \mathcal{H}_\ell) = P(x_i > \tau_1 | \mathcal{H}_\ell)$, $P(\bar{u}_i = -1 | u_i = -u_j = 1, \mathcal{H}_\ell) = P(\tau < x_i < \tau_1 | \mathcal{H}_\ell)$, $P(\bar{u}_i = 1 | u_i = -u_j = -1, \mathcal{H}_\ell) = P(\tau_2 < x_i < \tau | \mathcal{H}_\ell)$, $P(\bar{u}_i = -1 | u_i = -u_j = -1, \mathcal{H}_\ell) = P(x_i < \tau_2 | \mathcal{H}_\ell)$, respectively, are equal to $P_{d_1}, P_{d_2}, P_{d_3}, P_{d_4}$ under \mathcal{H}_1 , and are equal to $P_{f_1}, P_{f_2}, P_{f_3}, P_{f_4}$ under \mathcal{H}_0 . Since sensing noises are identically distributed and uncorrelated we find $P(F_{n_1, m_1} | \mathcal{H}_1) = \prod_{j=1}^4 P_{d_j}^{Q_{n_1, m_1}^j}$

and $P(F_{n_1, m_1} | \mathcal{H}_0) = \prod_{j=1}^4 P_{f_j}^{Q_{n_1, m_1}^j}$. Note that the relationship between $P_{e_1|h}, \mathcal{T}_{e_1|h}$ in (23) and $P_{e_2|h}, \mathcal{T}_{e_2|h}$ in (24) hold true. Using similar techniques in sections VI-A and VI-B we can establish the following

$$\bar{\mathcal{T}}_{e_1} < \frac{\mathbf{1}_{\{d_{n,m} \in S_0\}}}{2\sqrt{|S_1|}} \sum_{d_{n_1, m_1} \in S_1} [\sqrt{G(n, m, n_1, m_1)} \prod_{s=1}^S \mathcal{D}_1(n, m, n_1, m_1)] + \mathbf{1}_{\{d_{n,m} \in S_1\}}, \quad (42)$$

$$\bar{\mathcal{T}}_{e_2} < \frac{\mathbf{1}_{\{d_{n,m} \in S_1\}}}{|S_0|} \sum_{d_{n,m} \in S_0} [\min_t (|S_0| G(n, m, n_1, m_1))^t \prod_{s=1}^S \mathcal{D}_2(n, m, n_1, m_1)] + \mathbf{1}_{\{d_{n,m} \in S_0\}}, \quad (43)$$

in which $S_0 = \{d_{n_1, m_1} \text{ where } \frac{\prod_{j=1}^4 P_{d_j}^{Q_{n_1, m_1}^j}}{\prod_{j=1}^4 P_{f_j}^{Q_{n_1, m_1}^j}} < \frac{\pi_0}{\pi_1}\}$ and $S_1 = \{d_{n_1, m_1} \text{ where } \frac{\prod_{j=1}^4 P_{d_j}^{Q_{n_1, m_1}^j}}{\prod_{j=1}^4 P_{f_j}^{Q_{n_1, m_1}^j}} > \frac{\pi_0}{\pi_1}\}$ and

$$G(n, m, n_1, m_1) = \frac{(\pi_1 \prod_{j=1}^4 P_{d_j}^{Q_{n_1, m_1}^j} - \pi_0 \prod_{j=1}^4 P_{f_j}^{Q_{n_1, m_1}^j})}{(\pi_1 \prod_{j=1}^4 P_{d_j}^{Q_{n_1, m_1}^j} - \pi_0 \prod_{j=1}^4 P_{f_j}^{Q_{n_1, m_1}^j})}, \quad (44)$$

$$\mathcal{D}_1(n, m, n_1, m_1) = \left(\left(1 + \frac{\alpha \bar{\gamma}_h \bar{a}_1}{8}\right) \left(1 + \frac{\alpha \bar{\gamma}_h \bar{a}_2}{8}\right) - \frac{\alpha^2 \bar{\gamma}_h^2 \bar{a}_3}{64} \right)^{-1} \quad (45)$$

$$\mathcal{D}_2(n, m, n_1, m_1) = \left(\left(1 + \frac{\alpha(t^2 - t) \bar{\gamma}_h \bar{a}_1}{2}\right) \left(1 + \frac{\alpha(t^2 - t) \bar{\gamma}_h \bar{a}_2}{2}\right) - \frac{\alpha^2 (t^2 - t)^2 \bar{\gamma}_h^2 \bar{a}_3}{16} \right)^{-1} \quad (46)$$

$$\bar{a}_1 = (a_n^{2s-1} - a_{n_1}^{2s-1})^2 + (a_m^{2s} - a_{m_1}^{2s})^2, \quad \bar{a}_2 = (a_m^{2s-1} - a_{m_1}^{2s-1})^2 + (a_n^{2s} - a_{n_1}^{2s})^2$$

$$\bar{a}_3 = (a_n^{2s-1} - a_{n_1}^{2s-1})(a_m^{2s} - a_{m_1}^{2s}) - (a_m^{2s-1} - a_{m_1}^{2s-1})(a_n^{2s} - a_{n_1}^{2s}).$$

This completes our derivations for the upper bounds on $\bar{\mathcal{T}}_{e_1}, \bar{\mathcal{T}}_{e_2}$ and thus $\bar{P}_{e_1}, \bar{P}_{e_2}$. The upper bound on $\bar{\mathcal{T}}_{e_2}$ depends on t . Our simulations indicate that the bound is minimized for $t \approx 0.3$.

E. Comparison of Different Schemes in Asymptotic Regime for Large S

For all four schemes discussed in sections VI-A, VI-B, VI-C, VI-D, from sections A, B, C, D of Appendix B we have established the following, for large S

$$\bar{P}_e = \bar{P}_{e_1} + \bar{P}_{e_2} < \kappa_{l_{11}} e^{S(\mu_{l_{11}} + \frac{1}{2}\sigma_{l_{11}}^2)} + \frac{1}{2} e^{-S \frac{\mu_{l_{12}}^2}{2\sigma_{l_{12}}^2}} + \kappa_{l_{21}} e^{S(\mu_{l_{21}} + \frac{1}{2}\sigma_{l_{21}}^2)} + \frac{1}{2} e^{-S \frac{\mu_{l_{22}}^2}{2\sigma_{l_{22}}^2}},$$

$$\text{where } \mu_{l_{11}} + \frac{1}{2}\sigma_{l_{11}}^2, \mu_{l_{21}} + \frac{1}{2}\sigma_{l_{21}}^2 < 0.$$

Also, $\mu_{l_{11}}, \mu_{l_{12}}, \mu_{l_{21}}, \mu_{l_{22}}$ and $\sigma_{l_{11}}^2, \sigma_{l_{12}}^2, \sigma_{l_{21}}^2, \sigma_{l_{22}}^2$ and $\kappa_{l_{11}}, \kappa_{l_{21}}$ differ for different schemes and do not depend on S (they only depend on $\text{SNR}_h, \text{SNR}_c$ defined in Section VII and π_0). For each scheme we examine these four exponentials and keep the dominant one. Let $\kappa_{l_x} e^{-S\gamma_x}$ for $x = a, b, c, d$ be the dominant exponent, respectively, for schemes discussed in sections VI-A, VI-B, VI-C, VI-D, where

$\gamma_x = \min\{-(\mu_{l_{11}} + \frac{1}{2}\sigma_{l_{11}}^2), \frac{\mu_{l_{12}}^2}{2\sigma_{l_{12}}^2}, -(\mu_{l_{21}} + \frac{1}{2}\sigma_{l_{21}}^2), \frac{\mu_{l_{22}}^2}{2\sigma_{l_{22}}^2}\}$ and κ_{l_x} be its corresponding multiplicative scalar. When comparing the error exponents of any pair of these four schemes, for instance schemes in sections VI-A, VI-B, we have $\lim_{S \rightarrow \infty} (\frac{\ln(\kappa_{l_a} e^{-S\gamma_a})}{S} - \frac{\ln(\kappa_{l_b} e^{-S\gamma_b})}{S}) = \gamma_b - \gamma_a$, implying that such a difference depends on $\text{SNR}_h, \text{SNR}_c, \pi_0$ only and does not change with S . This analysis suggests that our numerical findings in Section VII on performance comparison between different schemes should not vary much for large $S = \frac{K}{2}$. In fact, our simulation results show that performance comparison between different schemes, given $\text{SNR}_h, \text{SNR}_c, \pi_0$, remains the same for $K = 10, 14$ and 20 (due to lack of space we only include the results for $K = 20$ in Table IV).

VII. NUMERICAL RESULTS

In this section, we evaluate and compare performance of the proposed schemes in Sections III, IV, V, against the conventional scheme in Section II-B. For the sakes of presentation, we refer to the schemes in Sections II-B, III, IV, and V, respectively, as “parallel”, “STC@sensors”, and “fusion@sensors”, “threshold changing@sensors”. We consider $K = 10$ sensors ($S = 5$ groups of paired sensors). We assume that the sensing noises w_k are identically distributed, i.e., $\sigma_{w_k}^2 = \sigma_w^2$ and $\rho_{ij} = \rho$ characterizes the correlation. We define $\text{SNR}_c = -20 \log_{10} \sigma_w$ as SNR corresponding to sensing channels. We let the distances between the sensors and the FC $d = 10m$, the distances between the cooperative partners within each group $d_0 = 2m$, the variance of receiver noises $\sigma_v^2 = \sigma_\eta^2 = -50dBm$, the pathloss exponent $\varepsilon = 2$, and the antenna gain $\mathcal{G} = -30dB$. To make a fair comparison among different schemes, we enforce the sensors in all schemes to transmit the same power \mathcal{P} . In “STC@sensors” and “fusion@sensors” a sensor spends $(1 - \alpha)\mathcal{P}$ and $\alpha\mathcal{P}$, respectively, for communicating with its cooperative partner and with the FC, where α is different in these two schemes. We define $\text{SNR}_h = 10 \log_{10} \bar{\gamma}_h$, in which $\bar{\gamma}_h = \frac{\sigma_h^2}{\sigma_v^2} = \frac{\mathcal{P}\mathcal{G}}{d^\varepsilon \sigma_v^2}$. Our goal is to investigate the average error \bar{P}_e of “STC@sensors”, “fusion@sensors”, “threshold changing@sensors” against that of “parallel”, as SNR_h and SNR_c vary and identify different regimes in which these schemes outperform “parallel”. Note that, in “STC@sensors” and “fusion@sensors”, given SNR_h and SNR_c , average error \bar{P}_e depends on α , i.e., one would expect that there is an optimal power allocation α^* at which \bar{P}_e attains its minimum, given SNR_h and SNR_c . We start with investigating α^* .

Optimal power allocation when the FC employs LRT rule: We start with “STC@sensors”. Fig. 2(a) plots \bar{P}_e versus α for $\text{SNR}_h = 5dB, \text{SNR}_c = 2, 6, 10dB$ and $\pi_0 = 0.6$, assuming $\rho = 0$. We observe that $\alpha^* \approx 0.65$, regardless of the variations in SNR_c values. Fig. 2(b) plots \bar{P}_e versus α for $\text{SNR}_c =$

6dB, $\text{SNR}_h = 5, 10, 15\text{dB}$ and $\pi_0 = 0.6$, assuming $\rho = 0$. We observe that α^* increases as SNR_h (or equivalently $\bar{\gamma}_h$) increases, in particular, we obtain $\alpha^* \approx 0.6, 0.7, 0.8$, respectively for $\text{SNR}_h = 5\text{dB}, 10\text{dB}, 15\text{dB}$. These observations can be explained considering our analytical results in (23)-(29) of Section VI-A. Recall $T_{n,m}, T_{n_1,m_1}$ in (27) capture the errors during inter-node communication and depend on the average received SNR $\bar{\gamma}_{hs}$ corresponding to inter-node communication, which for $\sigma_\eta^2 = \sigma_v^2$ it reduces to $\bar{\gamma}_{hs} = (\frac{d}{d_0})^\varepsilon (1 - \alpha) \bar{\gamma}_h$. This implies that $G(n, m, n_1, m_1)$ is decoupled into two fractions, where the first fraction depends on SNR_c (through the local performance indices P_d, P_f) and the second one depends on $(\frac{d}{d_0})^\varepsilon (1 - \alpha) \bar{\gamma}_h$. On the other hand, the inverses of $\mathcal{D}_1(n, m, n_1, m_1), \mathcal{D}_2(n, m, n_1, m_1)$ depend on $\alpha \bar{\gamma}_h$ only, capturing the errors of sensor-FC communication channels. Due to this decoupling of the effective factors in the terms of \bar{P}_e , we expect that, α^* becomes insensitive to variations of SNR_c (for fixed d, d_0, SNR_h) and varies as SNR_h changes (for fixed d, d_0, SNR_c). For the scenario where the distance between cooperative partners is shorter than the distance between the nodes and the FC we expect $\alpha^* > 0.5$, i.e., a sensor spends a higher (lower) percentage of its transmit power for communicating with the FC (its cooperative partner). These observations are in agreement with the fact that the local information exchange in “STC@sensors” does not affect the local error probability $p_{e_i} = P(u_i = -1 | \mathcal{H}_1) \pi_1 + P(u_i = 1 | \mathcal{H}_0) \pi_0$ at \mathcal{S}_i (which depends on SNR_c through P_d, P_f); it rather provides a form of “decision diversity”, to mitigate the fading effect during sensor-FC communication, i.e., it improves the global performance \bar{P}_e at the FC via reducing the errors during inter-sensor and sensor-FC communication.

We continue with “fusion@sensors”. Fig. 3(a) plots \bar{P}_e versus α for $\text{SNR}_h = 5\text{dB}, \text{SNR}_c = 2, 6, 10\text{dB}$ and $\pi_0 = 0.6$, assuming $\rho = 0$. We observe that α^* increases as SNR_c increases, in particular, we obtain $\alpha^* \approx 0.6, 0.7, 0.8$, respectively, for $\text{SNR}_c = 2, 6, 10\text{dB}$. Comparing this trend with that of “STC@sensors” in Fig. 2(a) we notice that the schemes have different trends. Fig. 3(b) plots \bar{P}_e versus α for $\text{SNR}_c = 6\text{dB}, \text{SNR}_h = 5, 10, 15\text{dB}$ and $\pi_0 = 0.6$, assuming $\rho = 0$. We observe that α^* increases as SNR_h (or equivalently $\bar{\gamma}_h$) increases, in particular, we obtain $\alpha^* \approx 0.7, 0.7, 0.85$, respectively for $\text{SNR}_h = 5, 10, 15\text{dB}$. Comparing this trend with that of “STC@sensors” in Fig. 2(b) we observe that the schemes have similar trends. These observations can be explained considering our analytical results in (37),(38) of Section VI-C. Note that similar to “STC@sensors”, the inverses of $\mathcal{D}_1(n, n_1), \mathcal{D}_2(n, n_1)$ depend on $\alpha \bar{\gamma}_h$ only, capturing the errors of sensor-FC communication channels. However, the structure of $G(n, n_1)$ is different from that of $G(n, m, n_1, m_1)$ in “STC@sensors”. In particular, examining $G(n, n_1)$ reveals that this term depends on $P(\tilde{u}_{2s-1}, \tilde{u}_{2s} | \mathcal{H}_\ell)$ for all pairs $|\mathcal{H}_\ell$ given in (12), which as we mentioned in Section IV-B, it depends on SNR_c

(through P_d, P_f) as well as the average received SNR $\bar{\gamma}_{hs}$ corresponding to inter-node communication. This implies that, different from $G(n, m, n_1, m_1)$ in “STC@sensors”, the impacts of effective factors SNR_c and $(\frac{d}{d_0})^\varepsilon(1 - \alpha)\bar{\gamma}_h$ in $G(n, n_1)$ cannot be decoupled and hence α^* varies as SNR_c changes (for fixed d, d_0, SNR_h) or SNR_h changes (for fixed d, d_0, SNR_c). These observations are in agreement with the fact that the local information exchange in “fusion@sensors”, different from “STC@sensors”, affects the local error probability $p_{e_i} = P(\tilde{u}_i = -1 | \mathcal{H}_1)\pi_1 + P(\tilde{u}_i = 1 | \mathcal{H}_0)\pi_0$ at \mathcal{S}_i . Therefore, it improves the global performance \bar{P}_e at the FC via improving the local error probability at the sensors. As SNR_c decreases (for fixed d, d_0, SNR_h) the reliability of the initial decision u_i at \mathcal{S}_i (which is based on observation x_i) reduces, and hence the local information exchange is more needed to form the new decision \tilde{u}_i with higher reliability, where more local information exchange is translated into a higher (lower) percentage of transmit power for inter-node communication (sensor-FC communication) or equivalently smaller α^* .

Optimal power allocation when the FC employs majority rule: Similar observations are made when the FC employs the majority rule. Figs. 4(a) and 5(a), respectively, plot \bar{P}_e versus α , for “STC@sensors” and “fusion@sensors”, when $\text{SNR}_h = 5\text{dB}$, $\text{SNR}_c = 2, 6, 10\text{dB}$ and $\pi_0 = 0.6$. Figs. 4(b) and 5(b), respectively, plot \bar{P}_e versus α , for “STC@sensors” and “fusion@sensors”, when $\text{SNR}_c = 6\text{dB}$, $\text{SNR}_h = 5, 10, 15\text{dB}$ and $\pi_0 = 0.6$. Comparing Fig. 2(a) with Fig. 4(a), Fig. 3(a) with Fig. 5(a), Fig. 2(b) with Fig. 4(b), and Fig. 3(b) with Fig. 5(b), we can make similar observations regarding the variations of α^* as SNR_c or SNR_h change. For each scheme, when we compare the value of α^* for LRT and majority rules, given $d, d_0, \text{SNR}_c, \text{SNR}_h$, we find that α^* corresponding to the majority rule is larger than that of the LRT rule, i.e., a sensor spends a higher (lower) percentage of its transmit power for communicating with the FC (its cooperative partner). This is due to the fact that, the majority rule demodulates first the sensor-FC channel outputs to find the channel inputs, rather than using the channel outputs directly for fusion, resembling the concept of “hard versus soft decoding” in [23]. To compensate for the information loss due to demodulation and its negative impact on error, each sensor is required to invest higher percentage of its transmit power for communicating with the FC.

Performance comparison of different schemes: To validate our performance analysis in Section VI, Fig. (6) shows \bar{P}_e of “parallel”, “STC@sensors”, “fusion@sensors”, “threshold changing@sensors” versus SNR_h for $\text{SNR}_c = 6\text{dB}$ and $\pi_0 = 0.6$, to compare the analytical and Monte-Carlo simulation results. We obtain \bar{P}_e of “STC@sensors” and “fusion@sensors”, using α^* corresponding to SNR_h and SNR_c values. The figure demonstrates a good agreement between theory and simulation. It also shows that, different

from conventional communication systems, \bar{P}_e has an error floor at high SNR_h . This behavior is due to the fact that \bar{P}_e in our distributed detection system is dependent on SNR_h and SNR_c . In fact, had all communication channels were error-free, \bar{P}_e of “parallel” would be

$$\begin{aligned} \bar{P}_e &= \pi_1 P \left(\frac{P_d^n (1 - P_d)^{2S-n}}{P_f^n (1 - P_f)^{2S-n}} < \frac{\pi_0}{\pi_1} \right) + \pi_0 P \left(\frac{P_d^n (1 - P_d)^{2S-n}}{P_f^n (1 - P_f)^{2S-n}} > \frac{\pi_0}{\pi_1} \right) \\ &= \pi_1 \sum_{n=0}^{M-1} \frac{(2S)!}{(2S-n)!n!} P_d^n (1 - P_d)^{2S-n} + \pi_0 \sum_{n=M}^{2S} \frac{(2S)!}{(2S-n)!n!} P_f^n (1 - P_f)^{2S-n}, \end{aligned} \quad (47)$$

where M satisfies $\frac{P_d^M (1 - P_d)^{2S-M}}{P_f^M (1 - P_f)^{2S-M}} > \frac{\pi_0}{\pi_1}$. Equation (47) indicates that the error floor depends on SNR_c (through P_d, P_f), and as SNR_c reduces the error floor increases. Fig. (6) also shows that “parallel” and “STC@sensors” have similar error floors, whereas “fusion@sensors” has a lower error floor. These observations are in agreement with the fact that the local information exchange in “STC@sensors” improves \bar{P}_e via providing “decision diversity”, without changing the local error probability at \mathcal{S}_i (which depends on the reliability of u_i). On the other hand, the local information exchange in “fusion@sensors” improves \bar{P}_e via improving the local error probability at \mathcal{S}_i (which depends on the reliability of \tilde{u}_i). For moderate/high SNR_h where the errors during inter-sensor and sensor-FC communication are negligible, \bar{P}_e is governed by the local error probability at \mathcal{S}_i . Since the reliability of local decisions in “parallel” and “STC@sensors” are identical and the reliability of local decisions in “fusion@sensors” exceeds that of “parallel” and “STC@sensors”, we expect that “parallel” and “STC@sensors” have similar error floors, whereas “fusion@sensors” reaches a lower error floor and Fig. (6) confirms these.

Table I tabulates \bar{P}_e of “parallel”, “STC@sensors”, “fusion@sensors” and “threshold changing@sensors”, as SNR_h and SNR_c vary, for $\pi_0 = 0.6$ and $\rho = 0$, when the FC employs the LRT rule. To have a fair comparison among different schemes, we obtain \bar{P}_e of “STC@sensors” and “fusion@sensors”, using α^* corresponding to SNR_h and SNR_c values. Comparing “STC@sensors” and “parallel” we note that, for moderate SNR_h and moderate/high SNR_c , “STC@sensors” outperforms “parallel”, while the performance gain of “STC@sensors” decreases as SNR_c reduces. On the other hand, for low SNR_h “STC@sensors” performs worse than “parallel”, whereas for high SNR_h “parallel” and “STC@sensors” reach similar error floors. These observations agree with the fact that the local information exchange in “STC@sensors” improves \bar{P}_e via providing “decision diversity”, without changing the local error probability at \mathcal{S}_i (which depends on SNR_c). For moderate/high SNR_h the errors during inter-sensor and sensor-FC

communication are small and \bar{P}_e is mainly determined by SNR_c . Therefore, lowering SNR_c increases \bar{P}_e . On the other hand, for low SNR_h the errors during inter-sensor communication negatively impact the diversity gain of “STC@sensors”. Comparing “fusion@sensors” and “parallel” we note that, for low SNR_h they have similar performance, whereas for moderate/high SNR_h “fusion@sensors” outperforms “parallel” (regardless of SNR_c). In particular, for high SNR_h the error floor of “fusion@sensors” is smaller than that of “parallel”. These observations agree with the facts that for moderate/high SNR_h , \bar{P}_e is dominated by the local probability error at \mathcal{S}_i , and the local probability error of “fusion@sensors” is smaller than that of “parallel”. Comparing “threshold changing@sensors” and “parallel” we note that the local decisions in “threshold changing@sensors” have an enhanced reliability, due to the fact that u_i, \bar{u}_i at \mathcal{S}_i are obtained based on comparing the sensor’s observation x_i with three thresholds (instead of one). For moderate/high SNR_h “threshold changing@sensors” outperforms “parallel” (regardless of SNR_c). This observation can be explained as follows. In this SNR_h regime, \bar{P}_e is dominated by the local probability error at \mathcal{S}_i . Since the reliability of local decisions in “threshold changing@sensors” exceeds that of local decisions in “parallel” we expect that “threshold changing@sensors” outperforms “parallel”. Furthermore, “threshold changing@sensors” improves \bar{P}_e over “parallel”, via providing “decision diversity” through Alamouti’s STC. For low SNR_h “threshold changing@sensors” outperforms “parallel” only for low SNR_c . This is because in this regime two factors contribute to \bar{P}_e : unreliable local decisions and communication channel errors. Since “threshold changing@sensors” increases the reliability of local decisions, its performance exceeds that of “parallel”. On the other hand, for low SNR_h and moderate/high SNR_c , where the communication channel errors are the major contributors to \bar{P}_e , Alamouti’s STC introduces destructive signal interference and degrades performance of “threshold changing@sensors” with respect to “parallel”.

Table I also tabulates \bar{P}_e of “parallel”, “STC@sensors”, “fusion@sensors” and “threshold changing@sensors”, as SNR_h and SNR_c vary, for $\pi_0 = 0.7$ and $\rho = 0$, when the FC employs the LRT rule. Similar observations can be made as we compare “STC@sensors” and “fusion@sensors” against “parallel” for different SNR_h and SNR_c regimes, regardless of π_0 . However, when comparing “threshold changing@sensors” against “parallel” in low SNR_h , we note that the behavior changes as π_0 increases. In particular, for low SNR_h “threshold changing@sensors” outperforms “parallel” for low SNR_c when π_0 is smaller. As π_0 increases, “threshold changing@sensors” outperforms “parallel” for low/moderate SNR_c , i.e., for low SNR_h the range of SNR_c values over which “threshold changing@sensors” outperforms

“parallel” expands as π_0 increases. Overall, Table I indicates that, for low SNR_h and moderate/high SNR_c , the proposed schemes do not have an advantage over “parallel”. The exception is when π_0 is large enough ($\pi_0 \geq 0.7$), in which case “threshold changing@sensors” outperforms ”parallel”. On the other hand, for low SNR_h and low SNR_c “fusion@sensors” and “threshold changing@sensors” outperform “parallel”. For moderate/high SNR_h , regardless of SNR_c , the schemes ranked from lowest to highest \bar{P}_e are “threshold changing@sensors”, “fusion@sensors”, “STC@sensors” and “parallel”. Table II is similar to Table I, with the difference that the FC employs the majority rule. Comparing each of the schemes “STC@sensors”, ”fusion@sensors” and “threshold changing@sensors” against “parallel” for different SNR_h and SNR_c regimes, we observe similar trends for the majority and LRT rules. However, when we compare the schemes to rank them based on their \bar{P}_e we note the differences. In particular, for very high SNR_c , “STC@sensors” outperforms all the schemes, for high SNR_c none of the proposed schemes has an advantage over “parallel”, and for moderate/low SNR_c “fusion@sensors” outperforms all the schemes.

Impact of correlation on performance comparison: Table III tabulates \bar{P}_e of “parallel”, “STC@sensors”, “fusion@sensors” and “threshold changing@sensors”, as SNR_h and SNR_c vary, for $\pi_0 = 0.7$ and $\rho = 0.1, 0.2, 0.3, 0.5, 0.8$, when the FC employs the LRT rule. We observe that as ρ increases the performance gap between the proposed schemes and “parallel” reduces. This observation can be explained as follows. As we mentioned before, the performance advantage of “fusion@sensors” and “threshold changing@sensors” over “parallel”, when the FC employs the LRT rules, is mainly due to the fact that the local information exchange in “fusion@sensors” or three-threshold-based test at the sensors in “threshold changing@sensors” would enhance the reliability of the local decisions (compared with “parallel”) when Gaussian sensing noises are uncorrelated. As these noises become correlated and ρ increases, the increase in the reliability of the local decisions in “fusion@sensors” and “threshold changing@sensors” diminishes and thus these two schemes start to lose their performance gain over “parallel”. For $\rho \leq 0.2$ the observations made on the performance comparison among these schemes remain the same as $\rho=0$. When ρ varies between 0.2–0.3, “threshold changing@sensors” outperforms others for high SNR_h , “fusion@sensors” outperforms others for medium SNR_h , and “parallel” and “fusion@sensors” outperform others for low SNR_h (all regardless of SNR_c). When $\rho=0.5$ for high SNR_h and high SNR_c “threshold changing@sensors” outperforms others. For high SNR_h and medium/low SNR_c and for medium SNR_h (regardless of SNR_c) “fusion@sensors” outperforms others. For low SNR_h (regardless of SNR_c) “parallel” and “fusion@sensors” outperform others. When $\rho=0.8$ “threshold

changing@sensors” has an inferior performance, regardless of SNR_h and SNR_c . Table III also shows that²⁷ the performance degradation of “threshold changing@sensors” is pronounced, as ρ increases, compared with other schemes. Note that at $\rho=0$ “threshold changing@sensors” has the lowest error floor, whereas at $\rho=1$ all schemes have the same error floor. These imply that the rate of performance degradation of “threshold changing@sensors” must be higher than other schemes.

Impact of increasing K : Table IV tabulates \bar{P}_e of “parallel”, “STC@sensors”, “fusion@sensors” and “threshold changing@sensors”, as SNR_h and SNR_c vary, for $\pi_0 = 0.6, \rho = 0, K = 20$, when the FC employs the LRT rule. The observations made on the comparison between these scheme for $K = 10$ remain true.

Discussion on increasing number of cooperative partners in a group: To investigate how increasing number of partners impacts the performance, we consider a network of $K=4$ sensors. Suppose sensors are positioned on the circumference of a circle on $x-y$ plane, whose center is located at the origin and its diameter is $2\sqrt{2}m$, and \mathcal{S}_i is equally distant from \mathcal{S}_j and \mathcal{S}_k such that $d_{ij} = d_{ik} = 2m, d_{jk} = 2\sqrt{2}m$. Also, the FC is located above the origin (above $x-y$ plane), such that all sensors are at equal distance of $d=10m$ from the FC. Let “STC4@sensors”, “fusion4@sensors” and “threshold changing4@sensors”, respectively, refer to schemes (i), (ii), (iii) with 4 partners in one group and “STC@sensors”, “fusion@sensors” and “threshold changing@sensors”, respectively, refer to schemes (i), (ii), (iii) with 2 partners in one group (two groups in the network). Table V tabulates \bar{P}_e of all schemes as SNR_h and SNR_c vary, for $\pi_0 = 0.6, 0.7$ and $\rho = 0$, when the FC employs LRT rule. Comparing all these schemes, we observe that for low SNR_h either “parallel” or ”threshold changing@sensors” outperforms others (depending on SNR_c), whereas for moderate/high SNR_h “threshold changing@sensors” outperforms others, including “fusion4@sensors”. These observations suggest that no performance gain is achieved as the number of cooperative partners increases beyond 2. In the following we provide our intuitive reasoning on how we expect schemes (i),(ii),(iii) perform, as the number of cooperative partners in a group increases, assuming K and sensor placements are fixed. Going from “STC@sensors” to “STC4@sensors”, for a fixed transmit power per sensor \mathcal{P} , we expect the power consumption for inter-sensor communication $(1-\alpha)\mathcal{P}$ increases, as the average distances between sensors within a group increase. This leaves a sensor with a smaller power, i.e., smaller $\alpha\mathcal{P}$, for its communication with the FC. For moderate/high SNR_c , the relative performance of “STC@sensors” and “STC4@sensors” depends on \mathcal{P} value. Our simulations show that for $\mathcal{P} > 32\text{mW}$, $\alpha\mathcal{P}$ is large enough that “STC4@sensors” provides a larger “decision diversity gain”

than that of “STC@sensors” during sensor-FC communication, and thus the former outperforms the latter. For low SNR_c , however, these schemes have similar performance, since performance in this regime is limited by the reliability of local decisions at sensors (which are the same for both schemes). Overall, these imply that for wireless sensor networks that typically operate within $0.12 \leq \mathcal{P} \leq 36\text{mW}$ [27], increasing the number of cooperative partners in a group beyond 2 does not have much practical incentive. Similarly, going from “fusion@sensors” to “fusion4@sensors”, we expect $(1 - \alpha)\mathcal{P}$ increases, while $\alpha\mathcal{P}$ decreases. However, different from scheme (i), in scheme (ii) local information exchange affects the reliability of local decisions. Hence, the increase of the reliability of the local decisions in “fusion4@sensors” due to the increase of $(1 - \alpha)\mathcal{P}$ still compensates for a less reliable sensor-FC communication due to the decrease of $\alpha\mathcal{P}$, which leads to the observation that “fusion4@sensors” outperforms “fusion@sensors” for $\mathcal{P} \geq 10\text{mW}$. Going to “fusion6@sensors” for $K=6$, however, α decreases further, such that even for a large $\mathcal{P} \approx 40\text{mW}$, the unreliability of the sensor-FC communication due to the decrease of $\alpha\mathcal{P}$ leads to the observation that “fusion6@sensors” performs worse than “fusion@sensors” (see Table VI). We expect similar performance degradation as we increase the number of partners in a group beyond 6. Going from “threshold changing@sensors” to “threshold changing4@sensors”, the former outperforms the latter for all SNR_c and SNR_h . This is due to the fact that, as the number of cooperative partners in a group increases, the chance that the corresponding information matrix transmitted by this group to the FC deviates from the conventional orthogonal STC matrix increases, leading to destructive signal interference at the FC and diminishing the “decision diversity gain” of STC. We conjecture similar performance degradation as we increase the number of partners in a group beyond 4.

Homogeneous versus inhomogeneous sensor placement: We consider a network of $K = 4$ sensors, consisting of two groups, where sensors are positioned on the circumference of a circle on $x-y$ plane, whose center is located at the origin and its diameter is 20m. The distance between two sensors in each group is $d_0 = 2\text{m}$. For homogeneous placement, we assume that the FC is located at the origin and for inhomogeneous placement, we move the FC toward one of the groups, such that the distance between the FC and the two groups are 4m and 16m. Table VII tabulates \bar{P}_e of “parallel”, “STC@sensors”, “fusion@sensors” and “threshold changing@sensors”, as SNR_h and SNR_c vary, for $\pi_0 = 0.6$, $\rho = 0$, when the FC employs the LRT rule, for homogeneous and inhomogeneous placements. This table shows that our findings on comparison between different schemes is exactly the same as Table I, which was another example of a homogenous placement. On the other hand, for inhomogeneous placement, “threshold

changing@sensors” outperforms other schemes, regardless of \mathcal{P} and SNR_c values. Since “threshold²⁹ changing@sensors” has the lowest error floor among all schemes, when one group of sensors becomes closer to the FC, the enhanced reliability of the information delivered to the FC by this group leads to the superior performance of this scheme. Comparing “STC@sensors” and “parallel”, we note the former performs worse than the latter in inhomogeneous placement. Since “STC@sensors” and “parallel” have similar error floor, placing one group of sensors closer to the FC does not change the reliability of the information provided by this group to the FC in either schemes. However, since the other group of sensors becomes farther away from the FC, the quality of the information delivered to the FC by this group decreases (due to destructive signal interference of STC), leading to the inferior performance of “STC@sensors”.

VIII. CONCLUSIONS

For the problem of binary distributed detection in a wireless sensor network, we have proposed novel cooperative and parallel fusion architectures, to combat fading effects encountered in the conventional parallel fusion architecture. In particular, we have proposed: (i) cooperative fusion architecture with Alamouti’s STC scheme at sensors, (ii) cooperative fusion architecture with signal fusion at sensors, and (iii) parallel fusion architecture with local threshold changing at sensors. While there is a limited local information exchange among the sensors (1-bit message) in schemes (i) and (ii), there is no explicit information exchange in scheme (iii). For these schemes, we derived the optimal LRT and the suboptimal majority fusion rules and analyzed their performance, in terms of communication and sensing SNRs. Our numerical results show that, when the FC employs the LRT rule, unless for low communication SNR and moderate/high sensing SNR, performance improvement is feasible with the new cooperative and parallel fusion architectures, while scheme (iii) outperforms others. When the FC utilizes the majority rule, such improvement is possible, unless for high sensing SNR. In particular, for very high sensing SNR scheme (i) outperforms, whereas for moderate/low sensing SNR scheme (ii) outperforms others.

APPENDIX A

Upper Bounds on $\mathcal{T}_{e_1|h}$ in (23) and its average $\bar{\mathcal{T}}_{e_1}$: For $Q_n < M$ we have

$$\mathcal{T}_{e_1|h} = P\left(\sum_{d_{n_1,m_1} \in S_1} d_{n_1,m_1} > -\sum_{d_{n_1,m_1} \in S_0} d_{n_1,m_1} | F_{n,m}\right) < P\left(\sum_{d_{n_1,m_1} \in S_1} d_{n_1,m_1} > -d_{n,m} | F_{n,m}\right). \quad (48)$$

where the bound in (48) is obtained noting that $d_{n,m} \in S_0$ and $\sum_{d_{n_1,m_1} \in S_0} d_{n_1,m_1} < d_{n,m}$. To further bound (48) we define the interval x and the function φ as the following

$$x = \mathbb{E}\left\{ \sum_{d_{n_1,m_1} \in S_1} C_{n_1,m_1} d_{n_1,m_1} | F_{n,m} \right\}, \quad \varphi(x) = P\left(\sum_{d_{n_1,m_1} \in S_1} C_{n_1,m_1} d_{n_1,m_1} > -d_{n,m} | F_{n,m} \right). \quad (49)$$

where constants C_{n_1,m_1} take values in the interval $[0, |S_1|]$. Our numerical results suggest that for small $|S_1|$, φ is convex over x . Invoking the inequality $\varphi\left(\frac{\sum_{i=1}^n x_i}{n}\right) \leq \frac{\sum_{i=1}^n \varphi(x_i)}{n}$, where the points x_1, \dots, x_n belong to x [26], and letting $n = |S_1|$ and $x_i = \mathbb{E}\{|S_1| d_{n_1,m_1} | F_{n,m}\}$ for $i = 1, \dots, |S_1|$ we establish below

$$\begin{aligned} \varphi\left(\sum_{d_{n_1,m_1} \in S_1} \mathbb{E}\{d_{n_1,m_1} | F_{n,m}\} \right) &= \varphi\left(\frac{1}{|S_1|} \sum_{d_{n_1,m_1} \in S_1} \mathbb{E}\{|S_1| d_{n_1,m_1} | F_{n,m}\} \right) \\ &\leq \frac{1}{|S_1|} \sum_{d_{n_1,m_1} \in S_1} \varphi(\mathbb{E}\{|S_1| d_{n_1,m_1} | F_{n,m}\}). \end{aligned} \quad (50)$$

The inequality in (50) implies that the upper bound on $\mathcal{T}_{e_1|h}$ in (48) can be further bounded as

$$P\left(\sum_{d_{n_1,m_1} \in S_1} d_{n_1,m_1} > -d_{n,m} | F_{n,m} \right) \leq \frac{1}{|S_1|} \sum_{d_{n_1,m_1} \in S_1} P(|S_1| d_{n_1,m_1} > -d_{n,m} | F_{n,m}). \quad (51)$$

The new bound on $\mathcal{T}_{e_1|h}$ in (51) can be presented in closed-form, considering the definitions of $d_{n,m}$ and d_{n_1,m_1} in (21) and noting that, conditioned on $u_{2s-1}, u_{2s}, \hat{u}_{2s-1}, \hat{u}_{2s}$, the terms z_{2s-1}, z_{2s} are independent complex Gaussian RVs with the variance $\sigma^2 = (|h_{2s-1}|^2 + |h_{2s}|^2) \sigma_v^2$ and the means $\mu_{2s-1}^{n_1,m_1}, \mu_{2s}^{n_1,m_1}$ for d_{n_1,m_1} and $\mu_{2s-1}^{n,m}, \mu_{2s}^{n,m}$ for $d_{n,m}$. Mapping the noises $\delta_{ij}^1, \delta_{ij}^2$ in Section III-B into δ_s^1, δ_s^2 , we find

$$P(|S_1| d_{n_1,m_1} > -d_{n,m} | F_{n,m}) = P(\zeta(n, m, n_1, m_1) > -\ln(|S_1| G(n, m, n_1, m_1)) + I(n, m, n_1, m_1)), \quad (52)$$

where $G(n, m, n_1, m_1)$ is defined in (27) and $I(n, m, n_1, m_1) = \sum_{s=1}^S \mathcal{K}_s(n, m, n_1, m_1)$ in which

$$\begin{aligned} \mathcal{K}_s(n, m, n_1, m_1) &= \frac{1}{\sigma^2} (|\mu_{2s-1}^{n_1,m_1} - \mu_{2s-1}^{n,m}|^2 + |\mu_{2s}^{n_1,m_1} - \mu_{2s}^{n,m}|^2) \\ &= \frac{\alpha}{2\sigma_v^2} (|h_{2s-1}(a_{n_1}^{2s-1} - a_n^{2s-1}) + h_{2s}(a_{n_1}^{2s} - a_n^{2s})|^2 \\ &\quad + |h_{2s-1}(a_{m_1}^{2s-1} - a_m^{2s-1}) + h_{2s}(a_{m_1}^{2s} - a_m^{2s})|^2), \\ \zeta(n, m, n_1, m_1) &= \sum_{s=1}^S \theta_s(n, m, n_1, m_1) \\ \text{where } \theta_s(n, m, n_1, m_1) &= \frac{2}{\sigma^2} \Re\{\delta_s^1(\mu_{2s-1}^{n_1,m_1} - \mu_{2s-1}^{n,m})^* + \delta_s^2(\mu_{2s}^{n_1,m_1} - \mu_{2s}^{n,m})^*\}. \end{aligned}$$

Recall δ_s^1 and δ_s^2 are i.i.d zero mean complex Gaussian RVs with the variance σ^2 . Hence, $\zeta(n, m, n_1, m_1)$ is a zero mean Gaussian RV with the variance $2I(n, m, n_1, m_1)$. Thus we can express (52) as

$$P(|S_1|d_{n_1, m_1} > -d_{n, m}|F_{n, m}) = Q\left(\frac{-\ln(|S_1|G(n, m, n_1, m_1)) + I(n, m, n_1, m_1)}{\sqrt{2I(n, m, n_1, m_1)}}\right). \quad (53)$$

Note that $I(n, m, n_1, m_1)$ depends on the coefficients h_{2s-1}, h_{2s} , whereas $G(n, m, n_1, m_1)$ is independent of these coefficients. In fact, $G(n, m, n_1, m_1)$ depends on sensing channels through P_d, P_f and the average received SNR $\bar{\gamma}_{hs}$ corresponding to inter-node communication through $T_{n, m}, T_{n_1, m_1}$. One can verify that when $\pi_0 > \pi_1$, we have $-\ln(|S_1|G(n, m, n_1, m_1)) + I(n, m, n_1, m_1) > 0$. Combining (48), (51), (53), using the Chernoff bound of Q -function $Q(x) < \frac{1}{2}e^{-\frac{x^2}{2}}$ for $x > 0$, and also noting that $0 < e^{-\frac{(\ln(|S_1|G(n, m, n_1, m_1)))^2}{4I(n, m, n_1, m_1)}} < 1$ and thus can be dropped without decreasing the upper bound, we find

$$\mathcal{T}_{e_1|h} < \frac{\mathbf{1}_{\{Q_n < M\}}}{2\sqrt{|S_1|}} \sum_{d_{n_1, m_1} \in S_1} \sqrt{G(n, m, n_1, m_1)} e^{-\frac{I(n, m, n_1, m_1)}{4}} + \mathbf{1}_{\{Q_n \geq M\}}. \quad (54)$$

Finally, to find an upper bound on $\bar{\mathcal{T}}_{e_1}$ we need to take average of $e^{-\frac{I(n, m, n_1, m_1)}{4}}$ in (54) over h_{2s-1}, h_{2s} for $s = 1, \dots, S$. Since $h_{2s-1}, h_{2s} \sim \mathcal{CN}(0, \sigma_h^2)$ are i.i.d across the pairs we have

$$\mathbb{E}\left\{e^{-\frac{I(n, m, n_1, m_1)}{4}}\right\} = \prod_{s=1}^S \int_{h_{2s-1}} \int_{h_{2s}} e^{-\frac{\kappa_s(n, m, n_1, m_1)}{4}} e^{-\frac{(|h_{2s-1}|^2 + |h_{2s}|^2)}{\sigma_h^2}} d_{h_{2s-1}} d_{h_{2s}}. \quad (55)$$

After some calculations (55) is reduced to $\prod_{s=1}^S \mathcal{D}_1(n, m, n_1, m_1)$ where $\mathcal{D}_1(n, m, n_1, m_1)$ is given in (28). The upper bound on $\bar{\mathcal{T}}_{e_1}$ is obtained by substituting $e^{-\frac{I(n, m, n_1, m_1)}{4}}$ in (54) with $\prod_{s=1}^S \mathcal{D}_1(n, m, n_1, m_1)$. This completes our derivations for the upper bound on $\bar{\mathcal{T}}_{e_1}$.

Upper Bounds on $\mathcal{T}_{e_2|h}$ in (24) and its average $\bar{\mathcal{T}}_{e_2}$: For $Q_n > M$ we have

$$\mathcal{T}_{e_2|h} < P(d_{n, m} < - \sum_{d_{n_1, m_1} \in S_0} d_{n_1, m_1} | F_{n, m}) < \frac{1}{|S_0|} \sum_{d_{n_1, m_1} \in S_0} P(d_{n, m} < -|S_0|d_{n_1, m_1} | F_{n, m}).. \quad (56)$$

noting that $d_{n, m} \in S_1$ and $\sum_{d_{n_1, m_1} \in S_1} d_{n_1, m_1} > d_{n, m}$. The new bound on $\mathcal{T}_{e_2|h}$ in (56) can be found in closed-form, via examining the definitions of $d_{n, m}$ and d_{n_1, m_1} in (21) and noting that, conditioned on $u_{2s-1}, u_{2s}, \hat{u}_{2s-1}, \hat{u}_{2s}$, the terms z_{2s-1}, z_{2s} are independent complex Gaussian RVs with the variance $\sigma^2 = (|h_{2s-1}|^2 + |h_{2s}|^2)\sigma_v^2$ and the means $\mu_{2s-1}^{n_1, m_1}, \mu_{2s}^{n_1, m_1}$ for d_{n_1, m_1} and $\mu_{2s-1}^{n, m}, \mu_{2s}^{n, m}$ for $d_{n, m}$. Therefore

$$P(d_{n, m} < -|S_0|d_{n_1, m_1} | F_{n, m}) = P(\zeta(n, m, n_1, m_1) > -\ln(|S_0|G(n, m, n_1, m_1)) + I(n, m, n_1, m_1)). \quad (57)$$

Comparing (57), (52), it seems natural to write (57) in terms of Q -function and apply Chernoff bound to reach a bound. However, different from (52), when $\pi_0 > \pi_1$ we no longer have $-\ln(|S_0|G(n, m, n_1, m_1)) + I(n, m, n_1, m_1) > 0$. We use an alternative bound, which states $P(\sum_{s=1}^S x_s < a) < \min_{t>0} e^{ta} \prod_{s=1}^S \mathbb{E}\{e^{-tx_s}\}$ when x_1, \dots, x_S are independent RVs [26]. Combining (56), (57), letting $x_s = -\theta_s(n, m, n_1, m_1)$, $a = \ln(|S_0|G(n, m, n_1, m_1)) - I(n, m, n_1, m_1)$ in (57) and using the alternative bound, we find

$$\begin{aligned} \mathcal{T}_{e_2|h} &< \frac{\mathbf{1}_{\{Q_n > M\}}}{|S_0|} \\ &\times \sum_{d_{n_1, m_1} \in S_0} [\min_t e^{-tI(n, m, n_1, m_1)} (|S_0|G(n, m, n_1, m_1))^t \prod_{s=1}^S \mathbb{E}\{e^{t\theta_s(n, m, n_1, m_1)}\}] + \mathbf{1}_{\{Q_n \leq M\}}. \end{aligned} \quad (58)$$

Noting that $-\theta_s(n, m, n_1, m_1) \sim \mathcal{CN}(0, 2\mathcal{K}_s(n, m, n_1, m_1))$ and using the moment generating function results we find $\mathbb{E}\{e^{t\theta_s(n, m, n_1, m_1)}\} = e^{t^2\mathcal{K}_s(n, m, n_1, m_1)}$. This implies we can rewrite (58) as the following

$$\mathcal{T}_{e_2|h} < \frac{\mathbf{1}_{\{Q_n > M\}}}{|S_0|} \sum_{d_{n_1, m_1} \in S_0} [\min_t (|S_0|G(n, m, n_1, m_1))^t \prod_{s=1}^S e^{(t^2-t)\mathcal{K}_s(n, m, n_1, m_1)}] + \mathbf{1}_{\{Q_n \leq M\}}. \quad (59)$$

To find a bound on $\bar{\mathcal{T}}_{e_2}$ we need to take average of $e^{(t^2-t)\mathcal{K}_s(n, m, n_1, m_1)}$ in (59) over h_{2s-1}, h_{2s} . One can verify that this term is equal to $\mathcal{D}_2(n, m, n_1, m_1)$ in (29). The upper bound on $\bar{\mathcal{T}}_{e_2}$ is obtained by substituting $e^{(t^2-t)\mathcal{K}_s(n, m, n_1, m_1)}$ in (59) with (29). This completes our derivations for the bound on $\bar{\mathcal{T}}_{e_2}$.

APPENDIX B

We analyze in details the behavior of our upper bounds on the average error probability for large S . In short, our analysis shows that, the difference between the error exponents of any two schemes (of the four schemes) depends on SNR_h , SNR_c and π_0 only, and does not change with S (recall S is the number of two-sensor groups and $K = 2S$ is the total number of sensors in the network). Therefore, our findings on performance comparison between different schemes for $\rho = 0$ remain the same when S increases.

Our detailed analysis follows. First for the ease of notation we define several new random vectors as the following: let $d_s^{(P)}$ and $d_s'^{(P)}$ be two independent and identically distributed random vectors that have the same distribution as the random vector $[u_{2s-1}, u_{2s}]$; Let $d_s^{(i)}$ and $d_s'^{(i)}$ be two independent and identically distributed random vectors that have the same distribution as the random vector $[u_{2s-1}, u_{2s}, \hat{u}_{2s-1}, \hat{u}_{2s}]$; Let $d_s^{(ii)}$ and $d_s'^{(ii)}$ be two independent and identically distributed random vectors that have the same distribution as the random vector $[\tilde{u}_{2s-1}, \tilde{u}_{2s}]$; And let $d_s^{(iii)}$ and $d_s'^{(iii)}$ be two independent and identically distributed random vectors that have the same distribution as the random vector $[u_{2s-1}, u_{2s}, \bar{u}_{2s-1}, \bar{u}_{2s}]$.

A. Classical Parallel Fusion Architecture

Using the definitions of $P_{e_1|h}$ and $P_{e_2|h}$ in (28), \bar{P}_{e_1} and \bar{P}_{e_2} can be written as

$$\bar{P}_{e_1} = \pi_0 \sum_n \bar{T}_{e_1} P(F_n|\mathcal{H}_0), \quad \bar{P}_{e_2} = \pi_1 \sum_n \bar{T}_{e_2} P(F_n|\mathcal{H}_0) \quad (60)$$

where upper bounds on \bar{T}_{e_1} and \bar{T}_{e_2} are derived and $P(F_n|\mathcal{H}_1) = P_d^{Q_n}(1 - P_d)^{K-Q_n}$ and $P(F_n|\mathcal{H}_0) = P_f^{Q_n}(1 - P_f)^{K-Q_n}$ are obtained in Section VI.B. Substituting these into (60) we can write the following

$$\bar{P}_{e_1} < \bar{P}_{e_{11}} + \bar{P}_{e_{12}}, \quad \bar{P}_{e_2} < \bar{P}_{e_{21}} + \bar{P}_{e_{22}}$$

where

$$\begin{aligned} \bar{P}_{e_{11}} &= \sum_n \frac{\mathbf{1}_{\{Q_n < M\}}}{2\sqrt{|S_1|}} \sum_{d_{n_1} \in S_1} [\sqrt{G(n, n_1)} \prod_{s=1}^S \mathcal{D}_1(n, n_1)] \pi_0 P_f^{Q_n} (1 - P_f)^{K-Q_n} \\ \bar{P}_{e_{12}} &= \sum_n (\mathbf{1}_{\{Q_n > M\}}) \pi_0 P_f^{Q_n} (1 - P_f)^{K-Q_n} \\ \bar{P}_{e_{21}} &= \sum_n \frac{\mathbf{1}_{\{Q_n > M\}}}{|S_0|} \sum_{d_{n_0} \in S_0} [\min_t (|S_0| G(n, n_1))^t \prod_{s=1}^S \mathcal{D}_1(n, n_1)] \pi_1 P_d^{Q_n} (1 - P_1)^{K-Q_n} \\ &= \sum_n \frac{\mathbf{1}_{\{Q_n > M\}}}{|S_0|^{1-t_0}} \sum_{d_{n_0} \in S_0} [G(n, n_1)^{t_0} \prod_{s=1}^S \mathcal{D}_1(n, n_1)] \pi_1 P_d^{Q_n} (1 - P_1)^{K-Q_n} \\ \bar{P}_{e_{22}} &= \sum_n (\mathbf{1}_{\{Q_n < M\}}) \pi_1 P_d^{Q_n} (1 - P_d)^{K-Q_n} \end{aligned} \quad (61)$$

where t_0 is the value that minimizes $\bar{P}_{e_{21}}$ in (61). Recall that $\bar{P}_{e_{12}}$ and $\bar{P}_{e_{22}}$ are the error floors (due to sensing noises), when communication channel is error-free. In the following, we discuss $\bar{P}_{e_{12}}$, $\bar{P}_{e_{11}}$, $\bar{P}_{e_{22}}$, $\bar{P}_{e_{21}}$ in asymptotic regime, as $S \rightarrow \infty$. • $\bar{P}_{e_{12}}$: we have $\bar{P}_{e_{12}} = P(L_{12} > \frac{\pi_0}{\pi_1} | \mathcal{H}_0)$ where the continuous random variable $L_{12} = \prod_{s=1}^S \frac{f(d_s^{(P)}|\mathcal{H}_1)}{f(d_s^{(P)}|\mathcal{H}_0)}$. Therefore $\ln L_{12} = \sum_{s=1}^S L_{s_{12}}$, where the continuous random variable $L_{s_{12}} = \ln(\frac{f(d_s^{(P)}|\mathcal{H}_1)}{f(d_s^{(P)}|\mathcal{H}_0)})$. Since $L_{s_{12}}$'s are i.i.d random variables with mean $\mu_{l_{12}} = \mathbb{E}_{d_s^{(P)}|\mathcal{H}_0}\{L_{s_{12}}\}$ and variance $\sigma_{l_{12}}^2 = \text{VAR}_{d_s^{(P)}|\mathcal{H}_0}(L_{s_{12}})$ that do not depend on s , we invoke the central limit theorem for large S to obtain

$$\bar{P}_{e_{12}} = Q\left(\frac{S\mu_{l_{12}} - \ln(\frac{\pi_0}{\pi_1})}{\sigma_{l_{12}}\sqrt{S}}\right) \approx Q\left(\frac{\sqrt{S}\mu_{l_{12}}}{\sigma_{l_{12}}}\right) < \underbrace{\kappa_{l_{12}}}_{=1/2} e^{-S\frac{\mu_{l_{12}}^2}{\sigma_{l_{12}}^2}}$$

- $\bar{P}_{e_{11}}$: After some tedious but straightforward mathematical manipulations, we reach

$$\begin{aligned}
\bar{P}_{e_{11}} &\stackrel{(a)}{=} \sum_n \frac{\mathbf{1}_{\{Q_n < M\}}}{2\sqrt{|S_1|}} \\
&\times \sum_{d_{n_1} \in S_1} \left[\frac{1 - \frac{\pi_0 P_f^{Q_{n_1}} (1-P_f)^{K-Q_{n_1}}}{\pi_1 P_d^{Q_{n_1}} (1-P_d)^{K-Q_{n_1}}}}{1 - \frac{\pi_1 P_d^{Q_n} (1-P_d)^{K-Q_n}}{\pi_1 P_f^{Q_n} (1-P_f)^{K-Q_n}}} \sqrt{\pi_0 P_f^{Q_n} (1-P_f)^{K-Q_n}} \sqrt{\pi_1 P_d^{Q_{n_1}} (1-P_d)^{K-Q_{n_1}}} \prod_{s=1}^S \mathcal{D}_1(n, n_1) \right] \\
&\stackrel{(b)}{<} \frac{1}{2\sqrt{|S_1|}} \frac{1}{\sqrt{1 - \frac{\pi_1 P_d^{M-1} (1-P_d)^{K-M+1}}{\pi_1 P_f^{M-1} (1-P_f)^{K-M+1}}}} \sum_n \sum_{n_1} \sqrt{\pi_0 P_f^{Q_n} (1-P_f)^{K-Q_n}} \sqrt{\pi_1 P_d^{Q_{n_1}} (1-P_d)^{K-Q_{n_1}}} \prod_{s=1}^S \mathcal{D}_1(n, n_1) \\
&\stackrel{(c)}{=} \underbrace{\frac{\sqrt{\pi_0 \pi_1}}{2\sqrt{|S_1|}} \frac{1}{\sqrt{1 - \frac{\pi_1 P_d^{M-1} (1-P_d)^{K-M+1}}{\pi_0 P_f^{M-1} (1-P_f)^{K-M+1}}}}}_{=\kappa_{l_{11}}} \\
&\sum_{a_n} \sum_{a_{n_1}} \left(\prod_{s=1}^S P(u_{2s-1} = a_n^{2s-1}, u_{2s} = a_{n_1}^{2s} | \mathcal{H}_0) P(u_{2s-1} = a_{n_1}^{2s-1}, u_{2s} = a_n^{2s} | \mathcal{H}_1) \right. \\
&\times \left. \prod_{s=1}^S \frac{\mathcal{D}_1(n, n_1)}{\sqrt{P(u_{2s-1} = a_n^{2s-1}, u_{2s} = a_n^{2s} | \mathcal{H}_0)} \sqrt{P(u_{2s-1} = a_{n_1}^{2s-1}, u_{2s} = a_{n_1}^{2s} | \mathcal{H}_1)}} \right) \quad (62)
\end{aligned}$$

where (a) follows by substituting $G(n, n_1)$ from Section VI.B in $\bar{P}_{e_{11}}$, (b) follows from the fact that the added terms in the righthand side of the inequality are all positive, $\frac{\pi_1 P_d^{Q_n} (1-P_d)^{K-Q_n}}{\pi_1 P_f^{Q_n} (1-P_f)^{K-Q_n}} < \frac{\pi_1 P_d^{M-1} (1-P_d)^{K-M+1}}{\pi_0 P_f^{M-1} (1-P_f)^{K-M+1}} < 1$, $Q_n < M$ and also $0 < \frac{\pi_0 P_f^{Q_{n_1}} (1-P_f)^{K-Q_{n_1}}}{\pi_1 P_d^{Q_{n_1}} (1-P_d)^{K-Q_{n_1}}} < 1$ when $d_{n_1} \in S_1$, and (c) follows from the substitution $P_f^{Q_n} (1-P_f)^{K-Q_n} = \prod_{s=1}^S (P(u_{2s-1} = a_n^{2s-1}, u_{2s} = a_n^{2s} | \mathcal{H}_0))$ and $P_d^{Q_{n_1}} (1-P_d)^{K-Q_{n_1}} = \prod_{s=1}^S (P(u_{2s-1} = a_{n_1}^{2s-1}, u_{2s} = a_{n_1}^{2s} | \mathcal{H}_1))$.

We define the discrete random variable L_{11} such that $\ln L_{11} = \sum_{s=1}^S L_{s_{11}}$, where the discrete random variable $L_{s_{11}} = \ln\left(\frac{D_1(d_s^{(P)}, d_s'^{(P)})}{\sqrt{P(d_s^{(P)} | \mathcal{H}_1)} \sqrt{P(d_s'^{(P)} | \mathcal{H}_0)}}\right)$. Our intuition behind defining the discrete random variable $L_{s_{11}}$ was that, $D_1(n, n_1)$ defined in Section VI.B, can be viewed as a realization of a discrete random variable. To find the corresponding random variable, we substitute $[a_n^{2s-1}, a_n^{2s}]$ and $[a_{n_1}^{2s-1}, a_{n_1}^{2s}]$, respectively, with $d_s^{(P)}$ and $d_s'^{(P)}$ in $D_1(n, n_1)$.

Note that the probability of the discrete random variable L_{11} assuming the particular value of $\prod_{s=1}^S \frac{D_1(n, n_1)}{\sqrt{P(u_{2s-1} = a_n^{2s-1}, u_{2s} = a_n^{2s} | \mathcal{H}_0)} \sqrt{P(u_{2s-1} = a_{n_1}^{2s-1}, u_{2s} = a_{n_1}^{2s} | \mathcal{H}_1)}}$ is equal to $\prod_{s=1}^S P(u_{2s-1} = a_n^{2s-1}, u_{2s} = a_n^{2s} | \mathcal{H}_0) P(u_{2s-1} = a_{n_1}^{2s-1}, u_{2s} = a_{n_1}^{2s} | \mathcal{H}_1)$. Hence (c) in (62) can be interpreted as calculating the

expectation of a random variable, that is

$$\bar{P}_{e_{11}} < \kappa_{l_{11}} \mathbb{E}_{d_1^{(P)}|\mathcal{H}_0, \dots, d_s^{(P)}|\mathcal{H}_0, d_1^{(P)}|\mathcal{H}_1, \dots, d_s^{(P)}|\mathcal{H}_1} \{L_{11}\}$$

Note that $L_{s_{11}}$'s are i.i.d random variable with mean $\mu_{l_{11}} = \mathbb{E}_{d_s^{(P)}|\mathcal{H}_0, d_s^{(P)}|\mathcal{H}_1} \{L_{s_{11}}\}$ and variance $\sigma_{l_{11}}^2 = \text{VAR}_{d_s^{(P)}|\mathcal{H}_0, d_s^{(P)}|\mathcal{H}_1} (L_{s_{11}})$ that do not depend on s . Also, we have verified that $\mu_{l_{11}} + \frac{1}{2}\sigma_{l_{11}}^2 < 0$. We invoke the central limit theorem for large S to say that $\ln L_{11}$ is a Gaussian random variable with mean $S\mu_{l_{11}}$ and variance $S\sigma_{l_{11}}^2$. This implies that L_{11} has log-normal distribution with mean $e^{S(\mu_{l_{11}} + \frac{1}{2}\sigma_{l_{11}}^2)}$, that is

$$\bar{P}_{e_{11}} < \kappa_{l_{11}} e^{S(\mu_{l_{11}} + \frac{1}{2}\sigma_{l_{11}}^2)}$$

- $\bar{P}_{e_{22}}$: Following similar steps as we took for calculating $\bar{P}_{e_{12}}$ for large S , we find

$$\bar{P}_{e_{22}} = \Phi\left(\frac{\sqrt{S}\mu_{l_{22}}}{\sigma_{l_{22}}}\right) = Q\left(-\frac{\sqrt{S}\mu_{l_{22}}}{\sigma_{l_{22}}}\right) < \underbrace{\kappa_{l_{22}}}_{=1/2} e^{-S\frac{\mu_{l_{22}}^2}{\sigma_{l_{22}}^2}}$$

where $\mu_{l_{22}} = \mathbb{E}_{d_s^{(P)}|\mathcal{H}_1} \{L_{s_{22}}\}$, $\sigma_{l_{22}}^2 = \text{VAR}_{d_s^{(P)}|\mathcal{H}_1} (L_{s_{22}})$ and the continuous random variable $L_{s_{22}} = \ln\left(\frac{f(d_s^{(P)}|\mathcal{H}_1)}{f(d_s^{(P)}|\mathcal{H}_0)}\right)$.

- $\bar{P}_{e_{21}}$: Following similar steps as we took for calculating $\bar{P}_{e_{11}}$ for large S , we find

$$\bar{P}_{e_{21}} < \underbrace{\frac{1}{|S_0|^{1-t_0}} \frac{\pi_0^{t_0} \pi_1^{1-t_0}}{\left(1 - \frac{\pi_0 P_f^M (1-P_f)^{K-M}}{\pi_1 P_d^M (1-P_d)^{K-M+1}}\right)^{t_0}}}_{=\kappa_{l_{21}}} e^{S(\mu_{l_{21}} + \frac{1}{2}\sigma_{l_{21}}^2)}$$

where $\mu_{l_{21}} = \mathbb{E}_{d_s^{(P)}|\mathcal{H}_1, d_s^{(P)}|\mathcal{H}_0} \{L_{s_{21}}\}$ and $\sigma_{l_{21}}^2 = \text{VAR}_{d_s^{(P)}|\mathcal{H}_1, d_s^{(P)}|\mathcal{H}_0} (L_{s_{21}})$ and the discrete random variable $L_{s_{21}} = \ln\left(\frac{D_2(d_s^{(P)}, d_s^{(P)})}{(P(d_s^{(P)}|\mathcal{H}_0))^{1-t_0} (P(d_s^{(P)}|\mathcal{H}_1))^{t_0}}\right)$. Also, we have verified that $\mu_{l_{21}} + \frac{1}{2}\sigma_{l_{21}}^2 < 0$. To find the discrete random variable $D_2(d_s^{(P)}, d_s^{(P)})$ we substitute $[a_n^{2s-1}, a_n^{2s}]$ and $[a_{n_1}^{2s-1}, a_{n_1}^{2s}]$, respectively, with $d_s^{(P)}$ and $d_s^{(P)}$ in $D_2(n, n_1)$ of Section VI.B.

B. Cooperative Fusion Architecture with STC at Sensors

Following similar steps as Section A above, we redefine $\bar{P}_{e_{11}}$, $\bar{P}_{e_{12}}$, $\bar{P}_{e_{21}}$ and $\bar{P}_{e_{22}}$ and write the following

$$\bar{P}_{e_1} < \bar{P}_{e_{11}} + \bar{P}_{e_{12}}, \quad \bar{P}_{e_2} < \bar{P}_{e_{21}} + \bar{P}_{e_{22}}$$

where

$$\begin{aligned}
\bar{P}_{e11} &= \sum_n \frac{\mathbf{1}_{\{Q_n < M\}}}{2\sqrt{|S_1|}} \sum_{d_{n_1, m_1} \in \mathcal{S}_1} [\sqrt{G(n, m, n_1, m_1)} \prod_{s=1}^S \mathcal{D}_1(n, m, n_1, m_1)] \pi_0 P_f^{Q_n} (1 - P_f)^{K - Q_n} \\
\bar{P}_{e12} &= \sum_n \mathbf{1}_{\{Q_n > M\}} \pi_0 P_f^{Q_n} (1 - P_f)^{K - Q_n} \\
\bar{P}_{e21} &= \sum_n \frac{\mathbf{1}_{\{Q_n > M\}}}{|S_0|} \sum_{d_{n_1, m_1} \in \mathcal{S}_0} [\min_t (|S_0| G(n, m, n_1, m_1))^t \prod_{s=1}^S \mathcal{D}_2(n, m, n_1, m_1)] \pi_0 P_f^{Q_n} (1 - P_f)^{K - Q_n} \quad (63) \\
&= \sum_n \frac{\mathbf{1}_{\{Q_n > M\}}}{|S_0|^{1-t_0}} \sum_{d_{n_1, m_1} \in \mathcal{S}_0} [G(n, m, n_1, m_1)^{t_0} \prod_{s=1}^S \mathcal{D}_2(n, m, n_1, m_1)] \pi_0 P_f^{Q_n} (1 - P_f)^{K - Q_n} \\
\bar{P}_{e22} &= \sum_n \mathbf{1}_{\{Q_n < M\}} \pi_1 P_d^{Q_n} (1 - P_d)^{K - Q_n}
\end{aligned}$$

where t_0 is the value that minimizes \bar{P}_{e21} in (63). Recall that \bar{P}_{e12} and \bar{P}_{e22} are the error floors, when communication channel is error-free. In the following, we discuss \bar{P}_{e12} , \bar{P}_{e11} , \bar{P}_{e22} , \bar{P}_{e21} in asymptotic regime, as $S \rightarrow \infty$.

- \bar{P}_{e12} : Since this scheme, i.e., scheme (i), has the same error floor as the scheme discussed in Section A above, \bar{P}_{e12} in this section is equal to \bar{P}_{e12} in Section A above.

- \bar{P}_{e11} : Following the same steps taken in Section A above for calculating \bar{P}_{e11} for large S , we find

$$\bar{P}_{e11} < \underbrace{\frac{\sqrt{\pi_0 \pi_1}}{2\sqrt{|S_1|}} \frac{1}{\sqrt{1 - \frac{\pi_1 P_d^{M-1} (1 - P_d)^{K-M+1}}{\pi_0 P_f^{M-1} (1 - P_f)^{K-M+1}}}}}_{=\kappa_{l11}} e^{S(\mu_{l11} + \frac{1}{2}\sigma_{l11}^2)}$$

where $\mu_{l11} = \mathbb{E}_{d_s^{(i)} | \mathcal{H}_0, d_s^{(i)} | \mathcal{H}_1} \{L_{s11}\}$, $\sigma_{l11}^2 = \text{VAR}_{d_s^{(i)} | \mathcal{H}_0, d_s^{(i)} | \mathcal{H}_1} (L_{s11})$ and the discrete random variable

$$L_{s11} = \ln \left(\frac{D_1(d_s^{(i)}, d_s^{\prime(i)})}{\sqrt{P(d_s^{(i)} | \mathcal{H}_1)} \sqrt{P(d_s^{(i)} | \mathcal{H}_0)}} \frac{P(\hat{u}'_{2s-1} | u'_{2s-1}) P(\hat{u}'_{2s} | u'_{2s})}{P(\hat{u}_{2s-1} | u_{2s-1}) P(\hat{u}_{2s} | u_{2s})} \right)$$

Also, we have verified that $\mu_{l11} + \frac{1}{2}\sigma_{l11}^2 < 0$. To find the discrete random variable $D_1(d_s^{(i)}, d_s^{\prime(i)})$ we substitute $[a_n^{2s-1}, a_n^{2s}, a_m^{2s-1}, a_m^{2s}]$ and $[a_{n_1}^{2s-1}, a_{n_1}^{2s}, a_{m_1}^{2s-1}, a_{m_1}^{2s}]$ respectively with $d_s^{(i)}$ and $d_s^{\prime(i)}$ in $D_1(n, m, n_1, m_1)$ in Section VI.A.

- \bar{P}_{e22} : Since this scheme, i.e., scheme (i), has the same error floor as the scheme discussed in Section A, \bar{P}_{e22} in this section is equal to \bar{P}_{e22} in Section A above.

- $\bar{P}_{e_{21}}$: Following the same steps taken in Section A for calculating $\bar{P}_{e_{21}}$ for large S , we find

$$\bar{P}_{e_{21}} < \underbrace{\frac{1}{|S_0|^{1-t_0}} \frac{\pi_0^t \pi_1^{1-t_0}}{\left(1 - \frac{\pi_0 P_f^M (1-P_f)^{K-M}}{\pi_1 P_d^M (1-P_d)^{K-M}}\right)^{t_0}}}_{=\kappa_{l_{21}}} e^{S(\mu_{l_{21}} + \frac{1}{2}\sigma_{l_{21}}^2)}$$

where $\mu_{l_{21}} = \mathbb{E}_{d_s^{(i)}|\mathcal{H}_1, d_s'^{(i)}|\mathcal{H}_0}\{L_{s_{21}}\}$, $\sigma_{l_{21}}^2 = \text{VAR}_{d_s^{(i)}|\mathcal{H}_1, d_s'^{(i)}|\mathcal{H}_0}(L_{s_{21}})$ and the discrete random variable

$$L_{s_{21}} = \ln\left(\frac{D_2(d_s^{(i)}, d_s'^{(i)})}{(P(d_s^{(i)}|\mathcal{H}_0))^{1-t_0} (P(d_s^{(i)}|\mathcal{H}_1))^{t_0}} \frac{(P(\hat{u}'_{2s-1}|u'_{2s-1})P(\hat{u}'_{2s}|u_{2s}))^{t_0}}{(P(\hat{u}_{2s-1}|u_{2s-1})P(\hat{u}_{2s}|u_{2s}))^{t_0}}\right)$$

Also, we verified that $\mu_{l_{21}} + \frac{1}{2}\sigma_{l_{21}}^2 < 0$. To find the discrete random variable $D_2(d_s^{(i)}, d_s'^{(i)})$ we substitute $[a_n^{2s-1}, a_n^{2s}, a_m^{2s-1}, a_m^{2s}]$ and $[a_{n_1}^{2s-1}, a_{n_1}^{2s}, a_{m_1}^{2s-1}, a_{m_1}^{2s}]$ respectively with $d_s^{(i)}$ and $d_s'^{(i)}$ in $D_2(n, m, n_1, m_1)$ of Section VI.A.

C. Cooperative Fusion Architecture with Signal Fusion at Sensors

Similar to previous sections, we redefine $\bar{P}_{e_{11}}$, $\bar{P}_{e_{12}}$, $\bar{P}_{e_{21}}$ and $\bar{P}_{e_{22}}$ and write the following

$$\bar{P}_{e_1} < \bar{P}_{e_{11}} + \bar{P}_{e_{12}}, \quad \bar{P}_{e_2} < \bar{P}_{e_{21}} + \bar{P}_{e_{22}}$$

where

$$\begin{aligned} \bar{P}_{e_{11}} &= \sum_n \frac{1 - \mathbf{1}_{\{Q_n^1, Q_n^2, Q_n^3\}}}{2\sqrt{|S_1|}} \sum_{d_{n_1} \in S_1} [\sqrt{G(n, n_1)} \prod_{s=1}^S (\mathcal{D}_1(n, n_1))] \pi_0 P(\tilde{u}_{2s-1} = a_n^{2s-1}, \tilde{u}_{2s} = a_n^{2s} | \mathcal{H}_0) \\ \bar{P}_{e_{12}} &= \sum_n (\mathbf{1}_{\{Q_n^1, Q_n^2, Q_n^3\}}) \pi_0 \prod_{s=1}^S P(\tilde{u}_{2s-1} = a_n^{2s-1}, \tilde{u}_{2s} = a_n^{2s} | \mathcal{H}_0) \\ \bar{P}_{e_{21}} &= \sum_n \frac{\mathbf{1}_{\{Q_n^1, Q_n^2, Q_n^3\}}}{(|S_0|)} \\ &\times \sum_{d_{n_1} \in S_1} [\min_t (|S_0| G(n, n_1))^t \prod_{s=1}^S (\mathcal{D}_1(n, n_1))] \pi_0 P(\tilde{u}_{2s-1} = a_n^{2s-1}, \tilde{u}_{2s} = a_n^{2s} | \mathcal{H}_1) \\ &= \sum_n \frac{\mathbf{1}_{\{Q_n^1, Q_n^2, Q_n^3\}}}{(|S_0|)^{1-t_0}} \sum_{d_{n_1} \in S_1} [G(n, n_1)^{t_0} \prod_{s=1}^S (\mathcal{D}_1(n, n_1))] \pi_0 P(\tilde{u}_{2s-1} = a_n^{2s-1}, \tilde{u}_{2s} = a_n^{2s} | \mathcal{H}_1) \\ \bar{P}_{e_{22}} &= \sum_n (1 - \mathbf{1}_{\{Q_n^1, Q_n^2, Q_n^3\}}) \pi_1 \prod_{s=1}^S P(\tilde{u}_{2s-1} = a_n^{2s-1}, \tilde{u}_{2s} = a_n^{2s} | \mathcal{H}_1) \end{aligned} \quad (64)$$

where t_0 is the value that minimizes $\bar{P}_{e_{21}}$ in (64). Recall that $\bar{P}_{e_{12}}$ and $\bar{P}_{e_{22}}$ are the error floors, when communication channel is error-free. In the following, we discuss $\bar{P}_{e_{12}}$, $\bar{P}_{e_{11}}$, $\bar{P}_{e_{22}}$, $\bar{P}_{e_{21}}$ in asymptotic

regime, as $S \rightarrow \infty$.

- \bar{P}_{e12} : Following the same steps taken in previous sections for calculating \bar{P}_{e12} for large S , we find

$$\bar{P}_{e12} \approx Q\left(\frac{\sqrt{S}\mu_{l12}}{\sigma_{l12}}\right) < \underbrace{\kappa_{l12}}_{=1/2} e^{-S\frac{\mu_{l12}^2}{\sigma_{l12}^2}}$$

where $\mu_{l12} = \mathbb{E}_{d_s^{(ii)}|\mathcal{H}_0}\{L_{s12}\}$, $\sigma_{l12}^2 = \text{VAR}_{d_s^{(ii)}|\mathcal{H}_0}(L_{s12})$ and the continuous random variable $L_{s12} = \ln\left(\frac{f(d_s^{(ii)}|\mathcal{H}_1)}{f(d_s^{(ii)}|\mathcal{H}_0)}\right)$.

- \bar{P}_{e11} : Following the same steps taken in previous sections for calculating \bar{P}_{e11} for large S , we find

$$\bar{P}_{e11} < \underbrace{\frac{1}{2\sqrt{|S_1|}} \frac{\sqrt{\pi_0\pi_1}}{\sqrt{1 - \text{LRT}_{\max}}}}_{=\kappa_{l11}} e^{S(\mu_{l11} + \frac{1}{2}\sigma_{l11}^2)} \quad (65)$$

where $\mu_{l11} = \mathbb{E}_{d_s^{(ii)}|\mathcal{H}_0, d_s'^{(ii)}|\mathcal{H}_1}\{L_{s11}\}$, $\sigma_{l11}^2 = \text{VAR}_{d_s^{(ii)}|\mathcal{H}_0, d_s'^{(ii)}|\mathcal{H}_1}(L_{s11})$ and the discrete random variable $L_{s11} = \ln\left(\frac{D_1(d_s^{(ii)}, d_s'^{(ii)})}{\sqrt{P(d_s^{(ii)}|\mathcal{H}_1)}\sqrt{P(d_s^{(ii)}|\mathcal{H}_0)}}\right)$. Also, we have verified that $\mu_{l11} + \frac{1}{2}\sigma_{l11}^2 < 0$. To find the discrete random variable $D_1(d_s^{(ii)}, d_s'^{(ii)})$ we substitute $[a_n^{2s-1}, a_n^{2s}]$ and $[a_{n_1}^{2s-1}, a_{n_1}^{2s}]$ respectively with $d_s^{(ii)}$ and $d_s'^{(ii)}$ in $D_1(n, n_1)$ of Section VI.C. Also, LRT_{\max} in (65) is

$$\begin{aligned} \text{LRT}_{\max} &= \max_n \left(\frac{\pi_1 \prod_{s=1}^S P(\tilde{u}_{2s-1} = a_n^{2s-1}, \tilde{u}_{2s} = a_n^{2s}|\mathcal{H}_1)}{\pi_0 \prod_{s=1}^S P(\tilde{u}_{2s-1} = a_n^{2s-1}, \tilde{u}_{2s} = a_n^{2s}|\mathcal{H}_0)} \right), \\ \text{given } &\frac{\pi_1 \prod_{s=1}^S P(\tilde{u}_{2s-1} = a_n^{2s-1}, \tilde{u}_{2s} = a_n^{2s}|\mathcal{H}_1)}{\pi_0 \prod_{s=1}^S P(\tilde{u}_{2s-1} = a_n^{2s-1}, \tilde{u}_{2s} = a_n^{2s}|\mathcal{H}_0)} < 1) \end{aligned}$$

- \bar{P}_{e22} : Following the same steps taken in previous sections for calculating \bar{P}_{e22} for large S , we find

$$\bar{P}_{e22} = \Phi\left(\frac{\sqrt{S}\mu_{l22}}{\sigma_{l22}}\right) < \underbrace{\kappa_{l22}}_{=1/2} e^{-S\frac{\mu_{l22}^2}{\sigma_{l22}^2}}$$

where $\mu_{l22} = \mathbb{E}_{d_s^{(ii)}|\mathcal{H}_1}\{L_{s22}\}$, $\sigma_{l22}^2 = \text{VAR}_{d_s^{(ii)}|\mathcal{H}_1}(L_{s22})$ and the continuous random variable $L_{s22} = \ln\left(\frac{f(d_s^{(ii)}|\mathcal{H}_1)}{f(d_s^{(ii)}|\mathcal{H}_0)}\right)$.

- \bar{P}_{e21} : Following the same steps taken in previous sections for calculating \bar{P}_{e21} for large S , we find

$$\bar{P}_{e21} < \underbrace{\frac{1}{(|S_0|)^{1-t_0} (1 - \text{LRT}_{\max})^{t_0}} \frac{\pi_0^{1-t_0} \pi_1^{t_0}}{}}_{=\kappa_{l21}} e^{S(\mu_{l21} + \frac{1}{2}\sigma_{l21}^2)}$$

where $\mu_{l21} = \mathbb{E}_{d_s^{(ii)}|\mathcal{H}_1, d_s'^{(ii)}|\mathcal{H}_0}\{L_{s21}\}$, $\sigma_{l21}^2 = \text{VAR}_{d_s^{(ii)}|\mathcal{H}_1, d_s'^{(ii)}|\mathcal{H}_0}(L_{s21})$ and the discrete random variable $L_{s21} = \ln\left(\frac{D_2(d_s^{(ii)}, d_s'^{(ii)})}{(P(d_s^{(ii)}|\mathcal{H}_0))^{1-t_0} (P(d_s^{(ii)}|\mathcal{H}_1))^{t_0}}\right)$. Also, we have verified that $\mu_{l21} + \frac{1}{2}\sigma_{l21}^2 < 0$. To find the

discrete random variable $D_2(d_s^{(ii)}, d_s'^{(ii)})$ we substitute $[a_n^{2s-1}, a_n^{2s}, a_m^{2s-1}, a_m^{2s}]$ and $[a_{n_1}^{2s-1}, a_{n_1}^{2s}, a_{m_1}^{2s-1}, a_{m_1}^{2s}]$ respectively with $d_s^{(i)}$ and $d_s'^{(i)}$ in $D_2(n, n_1)$ of Section VI.C.

D. Parallel Fusion Architecture with Local Threshold Changing at Sensors

Similar to previous sections, we redefine $\bar{P}_{e_{11}}$, $\bar{P}_{e_{12}}$, $\bar{P}_{e_{21}}$ and $\bar{P}_{e_{22}}$ and write the following

$$\bar{P}_{e_1} < \bar{P}_{e_{11}} + \bar{P}_{e_{12}}, \quad \bar{P}_{e_2} < \bar{P}_{e_{21}} + \bar{P}_{e_{22}}$$

where

$$\begin{aligned} \bar{P}_{e_{11}} &= \sum_{n,m} \frac{1 - \mathbf{1}_{\{Q_{n,m}^1, Q_{n,m}^2, Q_{n,m}^3\}}}{2\sqrt{|S_1|}} \sum_{d_{n_1, m_1} \in S_1} [\sqrt{G(n, m, n_1, m_1)} \prod_{s=1}^S (\mathcal{D}_1(n, m, n_1, m_1))] \\ &\times \pi_0 P(u_{2s-1} = a_n^{2s-1}, u_{2s} = a_n^{2s}, \bar{u}_{2s-1} = a_m^{2s-1}, \bar{u}_{2s} = a_m^{2s} | \mathcal{H}_0) \\ \bar{P}_{e_{12}} &= \sum_{n,m} (\mathbf{1}_{\{Q_{n,m}^1, Q_{n,m}^2, Q_{n,m}^3, Q_{n,m}^4\}}) \pi_0 \prod_{s=1}^S P(u_{2s-1} = a_n^{2s-1}, u_{2s} = a_n^{2s}, \bar{u}_{2s-1} = a_m^{2s-1}, \bar{u}_{2s} = a_m^{2s} | \mathcal{H}_0) \\ \bar{P}_{e_{21}} &= \sum_{n,m} \frac{\mathbf{1}_{\{Q_{n,m}^1, Q_{n,m}^2, Q_{n,m}^3\}}}{(|S_0|)} \sum_{d_{n_1, m_1} \in S_1} [\min_t (|S_0| G(n, m, n_1, m_1))^t \prod_{s=1}^S (\mathcal{D}_2(n, m, n_1, m_1))] \\ &\times \pi_1 P(u_{2s-1} = a_n^{2s-1}, u_{2s} = a_n^{2s}, \bar{u}_{2s-1} = a_m^{2s-1}, \bar{u}_{2s} = a_m^{2s} | \mathcal{H}_1) \\ &= \sum_{n,m} \frac{\mathbf{1}_{\{Q_{n,m}^1, Q_{n,m}^2, Q_{n,m}^3\}}}{(|S_0|)^{1-t_0}} \sum_{d_{n_1, m_1} \in S_1} [G(n, m, n_1, m_1)^{t_0} \prod_{s=1}^S (\mathcal{D}_2(n, m, n_1, m_1))] \\ &\times \pi_1 P(u_{2s-1} = a_n^{2s-1}, u_{2s} = a_n^{2s}, \bar{u}_{2s-1} = a_m^{2s-1}, \bar{u}_{2s} = a_m^{2s} | \mathcal{H}_1) \\ \bar{P}_{e_{22}} &= \sum_n (1 - \mathbf{1}_{\{Q_{n,m}^1, Q_{n,m}^2, Q_{n,m}^3, Q_{n,m}^4\}}) \pi_1 \prod_{s=1}^S P(u_{2s-1} = a_n^{2s-1}, u_{2s} = a_n^{2s}, \bar{u}_{2s-1} = a_m^{2s-1}, \bar{u}_{2s} = a_m^{2s} | \mathcal{H}_1) \end{aligned} \quad (66)$$

where t_0 is the value that minimizes $\bar{P}_{e_{21}}$ in (66). Recall that $\bar{P}_{e_{12}}$ and $\bar{P}_{e_{22}}$ are the error floors, when communication channel is error-free. In the following, we discuss $\bar{P}_{e_{12}}$, $\bar{P}_{e_{11}}$, $\bar{P}_{e_{22}}$, $\bar{P}_{e_{21}}$ in asymptotic regime, as $S \rightarrow \infty$.

- $\bar{P}_{e_{12}}$: Following the same steps taken in previous sections for calculating $\bar{P}_{e_{12}}$ for large S , we find

$$\bar{P}_{e_{12}} = Q\left(\frac{\sqrt{S}\mu_{l_{12}}}{\sigma_{l_{12}}}\right) < \underbrace{\kappa_{l_{12}}}_{=1/2} e^{-S \frac{\mu_{l_{12}}^2}{\sigma_{l_{12}}^2}}$$

where $\mu_{l_{12}} = \mathbb{E}_{d_s^{(iii)} | \mathcal{H}_0} \{L_{s_{12}}\}$, $\sigma_{l_{12}}^2 = \text{VAR}_{d_s^{(iii)} | \mathcal{H}_0} (L_{s_{12}})$ and the continuous random variable $L_{s_{12}} = \ln\left(\frac{f(d_s^{(iii)} | \mathcal{H}_1)}{f(d_s^{(iii)} | \mathcal{H}_0)}\right)$.

- \bar{P}_{e11} : Following the same steps taken in previous sections for calculating \bar{P}_{e11} for large S , we find

$$\bar{P}_{e11} < \underbrace{\frac{1}{2\sqrt{|S_1|}}}_{=\kappa_{l11}} \frac{\sqrt{\pi_0\pi_1}}{\sqrt{1-\text{LRT}_{\max}}} e^{S(\mu_{l11} + \frac{1}{2}\sigma_{l11}^2)} \quad (67)$$

where $\mu_{l11} = \mathbb{E}_{d_s^{(iii)}|\mathcal{H}_0, d_s'^{(iii)}|\mathcal{H}_1}\{L_{s11}\}$, $\sigma_{l11}^2 = \text{VAR}_{d_s^{(iii)}|\mathcal{H}_0, d_s'^{(iii)}|\mathcal{H}_1}(L_{s11})$ and discrete random variable $L_{s11} = \ln\left(\frac{D_1(d_s^{(iii)}, d_s'^{(iii)})}{\sqrt{P(d_s^{(iii)}|\mathcal{H}_1)}\sqrt{P(d_s^{(iii)}|\mathcal{H}_0)}}\right)$. Also, we have verified that $\mu_{l11} + \frac{1}{2}\sigma_{l11}^2 < 0$. To find the discrete random variable $D_1(d_s^{(iii)}, d_s'^{(iii)})$ we substitute $[a_n^{2s-1}, a_n^{2s}, a_m^{2s-1}, a_m^{2s}]$ and $[a_{n_1}^{2s-1}, a_{n_1}^{2s}, a_{m_1}^{2s-1}, a_{m_1}^{2s}]$ respectively with $d_s^{(i)}$ and $d_s'^{(i)}$ in $D_1(n, m, n_1, m_1)$ of Section VI.D. Also, LRT_{\max} in (67) is

$$\text{LRT}_{\max} = \max_{n, m} \left(\frac{\pi_1 \prod_{s=1}^S P(u_{2s-1} = a_n^{2s-1}, u_{2s} = a_n^{2s}, \bar{u}_{2s-1} = a_m^{2s-1}, \bar{u}_{2s} = a_m^{2s}|\mathcal{H}_1)}{\pi_0 \prod_{s=1}^S P(u_{2s-1} = a_n^{2s-1}, u_{2s} = a_n^{2s}, \bar{u}_{2s-1} = a_m^{2s-1}, \bar{u}_{2s} = a_m^{2s}|\mathcal{H}_0)} \right), \text{ given}$$

$$\frac{\pi_1 P(u_{2s-1} = a_n^{2s-1}, u_{2s} = a_n^{2s}, \bar{u}_{2s-1} = a_m^{2s-1}, \bar{u}_{2s} = a_m^{2s}|\mathcal{H}_1)}{\pi_0 P(u_{2s-1} = a_n^{2s-1}, u_{2s} = a_n^{2s}, \bar{u}_{2s-1} = a_m^{2s-1}, \bar{u}_{2s} = a_m^{2s}|\mathcal{H}_0)} < 1$$

- \bar{P}_{e22} : Following the same steps taken in previous sections for calculating \bar{P}_{e22} for large S , we find

$$\bar{P}_{e22} = \Phi\left(\frac{\sqrt{S}\mu_{l22}}{\sigma_{l22}}\right) < \underbrace{\kappa_{l22}}_{=1/2} e^{-S\frac{\mu_{l22}^2}{\sigma_{l22}^2}}$$

where $\mu_{l22} = \mathbb{E}_{d_s^{(iii)}|\mathcal{H}_1}\{L_{s22}\}$, $\sigma_{l22}^2 = \text{VAR}_{d_s^{(iii)}|\mathcal{H}_1}(L_{s22})$ and the continuous random variable $L_{s22} = \ln\left(\frac{f(d_s^{(iii)}|\mathcal{H}_1)}{f(d_s^{(iii)}|\mathcal{H}_0)}\right)$.

- \bar{P}_{e21} : Following the same steps taken in previous sections for calculating \bar{P}_{e21} for large S , we find

$$\bar{P}_{e21} < \underbrace{\frac{1}{(|S_0|)^{1-t_0}}}_{=\kappa_{l21}} \frac{\pi_0^{1-t_0} \pi_1^{t_0}}{(1-\text{LRT}_{\max})^{t_0}} e^{S(\mu_{l21} + \frac{1}{2}\sigma_{l21}^2)}$$

where $\mu_{l21} = \mathbb{E}_{d_s^{(iii)}|\mathcal{H}_1, d_s'^{(iii)}|\mathcal{H}_0}\{L_{s21}\}$, $\sigma_{l21}^2 = \text{VAR}_{d_s^{(iii)}|\mathcal{H}_1, d_s'^{(iii)}|\mathcal{H}_0}(L_{s21})$, and the discrete random variable $L_{s21} = \ln\left(\frac{D_2(d_s^{(iii)}, d_s'^{(iii)})}{(P(d_s^{(iii)}|\mathcal{H}_0))^{1-t_0}(P(d_s^{(iii)}|\mathcal{H}_1))^{t_0}}\right)$. Also, we have verified that $\mu_{l21} + \frac{1}{2}\sigma_{l21}^2 < 0$. To find the discrete random variable $D_2(d_s^{(iii)}, d_s'^{(iii)})$ we substituting $[a_n^{2s-1}, a_n^{2s}, a_m^{2s-1}, a_m^{2s}]$ and $[a_{n_1}^{2s-1}, a_{n_1}^{2s}, a_{m_1}^{2s-1}, a_{m_1}^{2s}]$ respectively with $d_s^{(i)}$ and $d_s'^{(i)}$ in $D_2(n, m, n_1, m_1)$ of Section VI.D.

REFERENCES

- [1] B. Chen, R. Jiang, T. Kasetkasem, and P. K. Varshney, "Channel aware decision fusion in wireless sensor networks," *IEEE Trans. Signal Processing*, vol. 52, no. 12, pp. 3454-3458, 2004.
- [2] R. Niu, B. Chen, and P. K. Varshney, "Fusion of decisions transmitted over Rayleigh fading channels in wireless sensor networks," *IEEE Trans. Signal Processing*, vol. 54, no. 3, pp. 1018-1027, 2006.

- [3] B. Chen, L. Tong and P.K. Varshney, "Channel-aware distributed detection in wireless sensor networks," *IEEE Signal Processing Magazine*, Vol. 23, pp 16-26, July 2006.
- [4] R. Jiang, S. Misra, B. Chen and A. Swami, "Robust suboptimal decision fusion in wireless sensor networks", *IEEE Proc. MILCOM*, October 2005.
- [5] H. Kim, J. Wang, P. Cai and S. Cui, "Detection Outage and Detection Diversity in a Homogeneous Distributed Sensor Network", *IEEE Trans. Signal Processing*, vol. 57, no. 7, pp. 2875-2881, 2009.
- [6] K. Lai, Y. Yang and J. Jia, "Fusion of Decisions Transmitted Over Flat Fading Channels Via Maximizing the Deflection Coefficient", *IEEE Trans. Vehicular Technology*, vol. 59, no. 7, pp. 3634- 3640, 2010.
- [7] J. Chamberland and V. V. Veeravalli, "Asymptotic results for decentralized detection in power constrained wireless sensor networks", *IEEE Journal on Selected Areas in Communications*, vol. 22, no. 6, pp. 1007 - 1015, 2004.
- [8] J. Chamberland and V. V. Veeravalli, "The impact of fading on decentralized detection in power constrained wireless sensor networks", *Proc. IEEE Intl. Conf. Acoust. Speech, Sig. Proc. (ICASSP)*, May 2004.
- [9] B. Chen and P. K. Willet, "On the optimality of the likelihood-ratio test for local sensor decision rules in the presence of nonideal channel", *IEEE Trans. on Information Theory*, vol. 51, pp. 693 - 699, 2005.
- [10] V.R. Kanchumathy, R. Viswanathan and M. Madishetty, "Impact of Channel Errors on Decentralized Detection Performance of Wireless Sensor Networks: A Study of Binary Modulations, Rayleigh-Fading and Nonfading Channels, and Fusion-Combiners", *IEEE Trans. Signal Processing*, vol. 56, no. 5, pp. 1761 -1769, 2008.
- [11] R. Jiang and B. Chen, "Fusion of censored decisions in wireless sensor networks", *IEEE Trans. on Wireless Communications*, vol. 4, no. 6, pp. 2668 - 2673, 2005.
- [12] A. Lei and R. Schober, "Multiple-symbol differential decision fusion for mobile wireless sensor networks," *IEEE Trans. on Wireless Communications*, vol. 9, no. 2, pp. 778-790, 2010.
- [13] J. N. Laneman, D. N. C. Tse, and G. W. Wornell, "Cooperative diversity in wireless networks: efficient protocols and outage behavior," *IEEE Trans. Information Theory*, vol. 50, no. 12, pp. 3062-3080, 2004.
- [14] P. F. Swaszek and P. Willett, "Parley as an approach to distributed detection," *IEEE Trans. Aerospace and Electronic Systems*, vol. 31, no. 1, pp. 447 -457, 1995.
- [15] D. Pados, K. W. Halford, D. Kazakos and P. Papantoni-Kazakos, "Distributed binary hypothesis testing with feedback," *IEEE Trans. Systems, Man and Cybernetics*, vol. 25, no. 1, pp. 21-42, 1995.
- [16] Y. W. Hong, A. Scaglione and P. K. Varshney, "A communication architecture for reaching consensus in decision for a large network," *IEEE Workshop on Statistical Signal Processing (SSP)*, 2005.
- [17] P. Braca, S. Marano, V. Matta and P. Willett, "Asymptotic Optimality of Running Consensus in Testing Binary Hypotheses," *IEEE Trans. Signal Processing*, vol. 58, no. 2, pp. 814-825, 2010.
- [18] Y. Jia and A. Vosoughi, "Impact of channel estimation error upon sum-rate in amplify-and-forward two-way relaying systems," *IEEE Workshop on Signal Processing Advances in Wireless Communications (SPAWC)*, 2010.
- [19] H. Ahmadi and A. Vosoughi, "Space-time coding for distributed detection in wireless sensor networks," *IEEE Workshop on Signal Processing Advances in Wireless Communications (SPAWC)*, 2009.
- [20] S. M. Alamouti, "A simple transmit diversity technique for wireless communications," *IEEE Journal on Selected Areas in Communications*, vol. 16, no. 8, pp. 1451-1458, 1998.

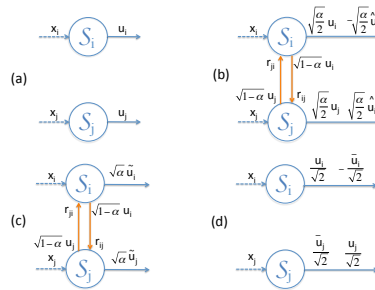


Fig. 1. (a) Conventional parallel fusion architecture, (b) cooperative fusion architecture with STC at sensors, (c) cooperative fusion architecture with signal fusion at sensors, (d) parallel fusion architecture with local threshold changing at sensors.

- [21] W. Zhang, K. B. Letaief, “Cooperative spectrum sensing with transmit and relay diversity in cognitive radio networks,” *IEEE Trans. Wireless Comm.*, vol. 7, no. 12, pp. 4761-4766, 2008.
- [22] N. Katenka, E. Levina, and G. Michailidis, “Local vote decision fusion for target detection in wireless sensor networks,” *IEEE Trans. Signal Processing*, vol. 56, pp. 329-338, 2008.
- [23] W. P. Tay, “The value of feedback in decentralized detection,” *IEEE Trans. Information Theory*, vol. 58, pp. 7226-7239, 2012.
- [24] O. P. Kreidl, J. N. Tsitsiklis, and S. I. Zoumpoulis, “On decentralized detection with partial information sharing among sensors,” *IEEE Trans. Signal Processing*, vol. 59, no. 4, pp. 1759-765, Apr. 2011.
- [25] H. Shalaby and A. Papamarcou, “A note on the asymptotics of distributed detection with feedback,” *IEEE Trans. Information Theory*, vol. 39, no. 2, pp. 633640, Mar. 1993.
- [26] Boyd and Vandenberghe, *Convex Optimization*, Cambridge university press, 2004.
- [27] V. Raghunathan, C. Schurgers, S. Park and M. B. Srivastava, “Energy-aware wireless microsensor networks,” *IEEE Signal Processing Magazine*, vol. 10, no. 2, pp. 40-50, Mar. 2002.

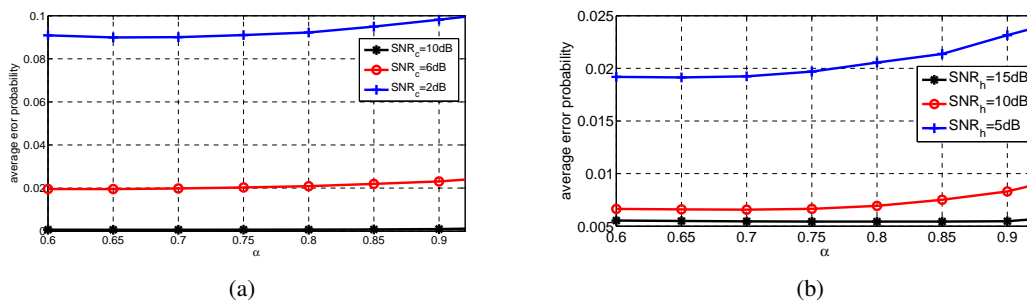


Fig. 2. “STC@sensors”: LRT rule (a) $SNR_h = 5\text{dB}$ with $SNR_c = 2, 6, 10\text{dB}$ (b) $SNR_c = 6\text{dB}$ with $SNR_h = 5, 10, 15\text{dB}$

TABLE I
ALL SCHEMES, LRT RULE, $\rho = 0$, $K = 10$

SNR _h	SNR _c = 10dB			SNR _c = 6dB			SNR _c = 2dB			
	5dB	10dB	15dB	5dB	10dB	15dB	5dB	10dB	15dB	
parallel	1.9e-4	3.8e-5	2.0e-5	1.2e-2	7.3e-3	5.6e-3	7.6e-2	6.6e-2	6.4e-2	$\pi_0 = 0.6$
STC	8.7e-4	3.1e-5	1.4e-5	1.8e-2	6.9e-3	5.4e-3	8.9e-2	6.5e-2	6.3e-2	
fusion	1.9e-4	1.7e-5	1.4e-5	1.2e-2	4.8e-3	3.9e-3	7.4e-2	5.5e-2	5.2e-2	
threshold	3.4e-4	1.7e-5	3.0e-6	1.2e-2	4.4e-3	2.6e-3	7.5e-2	4.7e-2	3.7e-2	
parallel	3.0e-4	4.3e-5	2.3e-5	1.3e-2	7.4e-3	6.7e-3	8.1e-2	7.0e-2	6.6e-2	$\pi_0 = 0.7$
STC	8.9e-4	2.9e-5	1.9e-5	1.9e-2	7.1e-3	6.2e-3	9.4e-2	6.9e-2	6.5e-2	
fusion	2.3e-4	2.0e-5	7e-6	1.3e-2	5.9e-3	5.4e-3	7.9e-2	5.9e-2	5.5e-2	
threshold	3.9e-4	1.5e-5	0.0e-6	1.2e-2	3.9e-3	2.4e-3	7.1e-2	4.6e-2	3.5e-2	

TABLE II
ALL SCHEMES, MAJORITY RULE, $\rho = 0$, $K = 10$

SNR _h	SNR _c = 13dB		SNR _c = 10dB			SNR _c = 6dB			SNR _c = 2dB			
	5dB	10dB	5dB	10dB	15dB	5dB	10dB	15dB	5dB	10dB	15dB	
parallel	2.4e-4	4e-6	1.3e-3	4.0e-5	9.0e-5	3.2e-2	2.2e-2	1.8e-2	1.4e-1	1.3e-1	1.3e-1	$\pi_0 = 0.6$
STC	1.4e-3	2e-6	4.2e-3	2.3e-4	6.0e-5	4.4e-2	2.0e-2	1.7e-2	1.5e-1	1.3e-1	1.3e-1	
fusion	1.7e-4	3e-6	1.3e-3	4.0e-5	3e-5	2.7e-2	1.3e-2	1.0e-2	1.2e-1	9.7e-2	9.0e-2	
threshold			2.4e-2	1.3e-2	1.1e-3	1.2e-1	1.0e-1	9.7e-2	2.3e-1	2.2e-1	2.1e-1	
parallel			2.0e-3	5.3e-5	2.0e-4	6.1e-2	4.2e-2	3.7e-2	2.0e-1	2.0e-1	2.0e-1	$\pi_0 = 0.7$
STC			4.9e-3	4.7e-4	1.6e-5	6.8e-2	3.9e-2	3.6e-2	1.9e-1	2.0e-1	2.0e-1	
fusion			1.2e-3	1.8e-4	6e-5	2.3e-2	1.4e-2	1.2e-2	9.2e-2	1.0e-1	9.8e-2	
threshold			2.2e-2	1.3e-2	1.0e-3	1.0e-1	9.6e-2	9.0e-2	2.0e-1	1.9e-1	1.9e-1	

TABLE III
ALL SCHEMES, LRT RULE, $\pi_0 = 0.7$, $K = 10$

SNR _h	SNR _c = 10dB			SNR _c = 6dB			SNR _c = 2dB			
	5dB	10dB	15dB	5dB	10dB	15dB	5dB	10dB	15dB	
parallel	7.4e-4	5.3e-4	3.8e-4	2.8e-2	2.4e-2	2.2e-2	1.10e-1	1.02e-1	9.95e-2	$\rho = 0.1$
STC	7.7e-4	4.3e-4	3.8e-4	3.2e-2	1.8e-2	2.0e-2	1.18e-1	1.02e-1	9.89e-2	
fusion	6.9e-4	3.0e-4	2.2e-4	2.5e-2	1.7e-2	1.6e-2	1.05e-1	9.5e-2	9.06e-2	
threshold	9.3e-4	2.2e-4	1.5e-4	2.6e-2	1.5e-2	1.3e-2	1.09e-1	8.7e-2	7.81e-2	
parallel	2.7e-3	1.9e-3	1.7e-3	4.0e-2	3.6e-2	3.5e-2	1.38e-1	1.32e-1	1.31e-1	$\rho = 0.2$
STC	3.4e-3	1.8e-3	1.6e-3	4.4e-2	3.5e-2	3.5e-3	1.43e-1	1.32e-1	1.32e-1	
fusion	2.5e-3	1.3e-3	1.1e-3	3.9e-2	3.3e-2	3.3e-2	1.37e-1	1.29e-1	1.25e-1	
threshold	3.1e-2	1.4e-3	1.0e-3	4.3e-2	3.4e-2	3.0e-2	1.42e-1	1.29e-1	1.24e-1	
parallel	4.8e-3	3.8e-3	3.5e-3	5.7e-2	5.2e-2	5.2e-2	1.60e-1	1.54e-1	1.54e-1	$\rho = 0.3$
STC	5.8e-3	3.5e-3	3.5e-3	6.0e-2	5.2e-2	5.1e-3	1.64e-1	1.56e-1	1.56e-1	
fusion	4.8e-3	3.4e-3	3.3e-3	5.6e-2	5.0e-2	4.9e-2	1.60e-1	1.52e-1	1.52e-1	
threshold	3.1e-2	3.5e-3	2.7e-3	6.1e-2	5.1e-2	4.9e-2	1.62e-1	1.54e-1	1.50e-1	
parallel	1.4e-2	1.4e-2	1.3e-2	9.19e-2	8.95e-2	8.99e-2	1.80e-1	1.77e-1	1.77e-1	$\rho = 0.5$
STC	1.6e-2	1.3e-2	1.3e-2	9.35e-2	8.97e-2	8.89e-2	1.79e-1	1.71e-1	1.71e-1	
fusion	1.4e-3	1.2e-2	1.2e-2	9.12e-2	8.79e-2	8.55e-2	1.72e-1	1.71e-1	1.71e-1	
threshold	1.4e-2	1.3e-2	1.0e-2	9.19e-2	8.80e-2	8.70e-2	1.80e-1	1.78e-1	1.77e-1	
parallel	3.1e-2	3.0e-2	2.9e-2	1.25e-1	1.25e-1	1.25e-1	2.10e-1	2.10e-1	2.09e-1	$\rho = 0.8$
STC	3.0e-2	2.8e-2	2.8e-2	1.25e-1	1.25e-1	1.25e-1	2.12e-1	2.09e-1	2.09e-1	
fusion	2.9e-2	2.9e-2	2.8e-2	1.25e-1	1.25e-1	1.25e-1	2.09e-1	2.09e-1	2.09e-1	
threshold	3.0e-2	3.0e-2	3.0e-2	1.29e-1	1.29e-1	1.29e-1	2.17e-1	2.20e-1	2.22e-1	

TABLE IV
ALL SCHEMES, LRT RULE, $\rho = 0$, $\pi_0 = 0.6$, $K = 20$

	SNR _c = 10dB			SNR _c = 6dB			SNR _c = 2dB		
	5dB	10dB	15dB	5dB	10dB	15dB	5dB	10dB	15dB
SNR _h									
parallel	3.8e-7	4.0e-8	3.0e-9	7.6e-4	3.3e-4	2.3e-4	2.3e-2	1.6e-2	1.5e-2
STC	3.8e-6	2.0e-8	2.0e-9	1.6e-3	2.6e-4	1.8e-4	2.7e-2	1.5e-2	1.3e-2
fusion	3.6e-7	5.7e-9	2.0e-9	6.0e-4	1.7e-4	9.5e-5	2.1e-2	1.3e-2	1.1e-2
threshold	8.5e-7	6.0e-9	1.0e-10	7.3e-4	1.1e-4	3.8e-5	2.1e-2	9.1e-3	6.0e-3

TABLE V
ALL SCHEMES FOR A GROUP OF FOUR SENSORS, LRT RULE, $\rho = 0$, $K = 4$

	SNR _c = 10dB			SNR _c = 6dB			SNR _c = 2dB			
	5dB	10dB	15dB	5dB	10dB	15dB	5dB	10dB	15dB	
SNR _h										
parallel	1.3e-2	5.9e-3	5.3e-3	7.3e-2	5.8e-2	5.6e-2	1.8e-1	1.5e-1	1.5e-1	$\pi_0 = 0.6$
STC4	6.1e-2	6.7e-3	5.1e-3	1.3e-1	6.0e-2	5.4e-2	1.5e-1	1.5e-1	1.5e-1	
fusion4	1.3e-2	2.8e-3	1.6e-3	7.8e-2	4.5e-2	3.7e-2	1.8e-1	1.4e-1	1.3e-1	
threshold4	2.8e-1	2.4e-1	2.0e-1	3.0e-1	2.7e-1	1.9e-1	3.9e-1	3.0e-1	2.2e-1	
STC	2.1e-2	5.8e-3	5.1e-3	8.8e-2	5.7e-2	5.4e-2	1.9e-1	1.5e-1	1.5e-1	
fusion	1.3e-2	3.8e-3	3.6e-3	7.4e-2	5.2e-2	4.9e-2	1.8e-1	1.5e-1	1.4e-1	
threshold	1.5e-2	2.8e-3	1.5e-3	7.8e-2	4.4e-2	3.5e-2	1.7e-1	1.3e-1	1.2e-1	
parallel	1.0e-2	5.5e-3	4.8e-3	6.7e-2	5.3e-2	5.0e-2	1.6e-1	1.5e-1	1.4e-1	$\pi_0 = 0.7$
STC4	5.7e-2	8.3e-3	3.5e-3	1.3e-1	5.8e-2	4.2e-2	2.0e-1	1.5e-1	1.4e-1	
fusion4	1.5e-2	4.5e-3	2.6e-3	8.2e-2	5.0e-2	4.4e-2	1.7e-1	1.4e-1	1.3e-1	
threshold4	2.3e-1	1.7e-1	2.0e-1	1.4e-1	2.0e-1	1.4e-1	2.9e-1	2.7e-1	1.2e-1	
STC	1.8e-2	5.0e-3	4.1e-3	7.9e-2	5.0e-2	4.8e-2	1.7e-1	1.4e-1	1.4e-1	
fusion	9.7e-3	4.6e-3	3.8e-3	6.7e-2	5.3e-2	4.7e-2	1.6e-1	1.4e-1	1.4e-1	
threshold	1.2e-2	3.1e-3	2.2e-3	7.0e-2	4.5e-2	3.4e-2	1.6e-1	1.3e-1	1.2e-1	

TABLE VI
“PARALLEL”, “FUSION@SENSORS” AND “FUSION6@SENSORS”, LRT RULE, $\rho = 0$, $\pi_0 = 0.6$, $K = 6$

	SNR _c = 10dB			SNR _c = 6dB			SNR _c = 2dB		
	5dB	10dB	15dB	5dB	10dB	15dB	5dB	10dB	15dB
SNR _h									
parallel	3.0e-3	1.3e-3	9.0e-4	3.7e-2	2.9e-2	2.7e-2	1.3e-1	1.1e-1	1.1e-1
fusion	2.8e-3	8.0e-4	3.0e-4	3.5e-2	2.1e-2	1.7e-2	1.2e-1	9.5e-2	9.0e-2
fusion6	3.1e-3	1.3e-3	3.1e-4	3.8e-2	2.9e-2	2.6e-2	1.4e-1	1.1e-1	9.9e-2

TABLE VII
ALL SCHEMES, LRT RULE, $\rho = 0$, $\pi_0 = 0.6$, $K = 4$

	SNR _c = 10dB			SNR _c = 6dB			SNR _c = 2dB			
	5dB	10dB	15dB	5dB	10dB	15dB	5dB	10dB	15dB	
SNR _h										
parallel	1.3e-2	5.9e-3	5.3e-3	7.3e-2	5.8e-2	5.6e-2	1.8e-1	1.5e-1	1.5e-1	homogenous
STC	2.1e-2	5.8e-3	5.1e-3	8.8e-2	5.7e-2	5.4e-2	1.9e-1	1.5e-1	1.5e-1	
fusion	1.3e-2	3.8e-3	3.6e-3	7.4e-2	5.2e-2	4.9e-2	1.8e-1	1.5e-1	1.4e-1	
threshold	1.5e-2	2.8e-3	1.5e-3	7.8e-2	4.4e-2	3.5e-2	1.7e-1	1.3e-1	1.2e-1	
\mathcal{P}	3.2mW	10mW	32mW	3.2mW	10mW	32mW	3.2mW	10mW	32mW	inhomogenous
parallel	1.1e-2	6.4e-3	5.2e-3	7.5e-2	6.0e-2	5.8e-2	1.7e-1	1.5e-1	1.5e-1	
STC	1.4e-2	6.9e-3	5.1e-3	8.4e-2	5.8e-2	5.6e-2	1.8e-1	1.5e-1	1.5e-1	
fusion	1.1e-2	4.0e-3	3.6e-3	7.3e-2	5.4e-2	4.9e-2	1.7e-1	1.5e-1	1.4e-1	
threshold	1.0e-2	3.6e-3	1.4e-3	6.3e-2	4.5e-2	3.3e-2	1.6e-1	1.4e-1	1.2e-1	

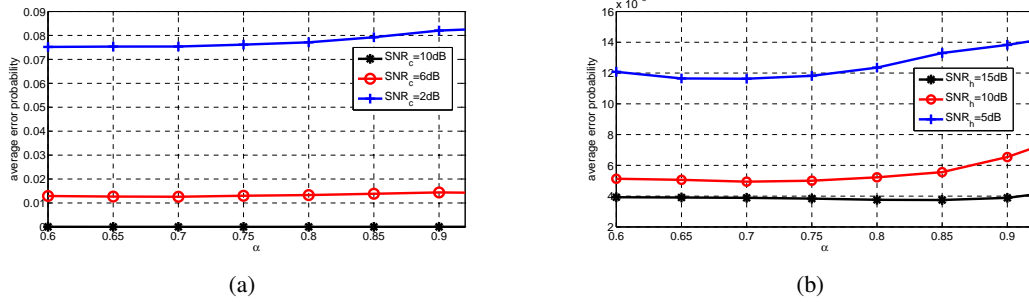


Fig. 3. “fusion@sensors”: LRT rule (a) $SNR_h=5\text{dB}$ with $SNR_c=2,6,10\text{dB}$ (b) $SNR_c=6\text{dB}$ with $SNR_h=5,10,15\text{dB}$

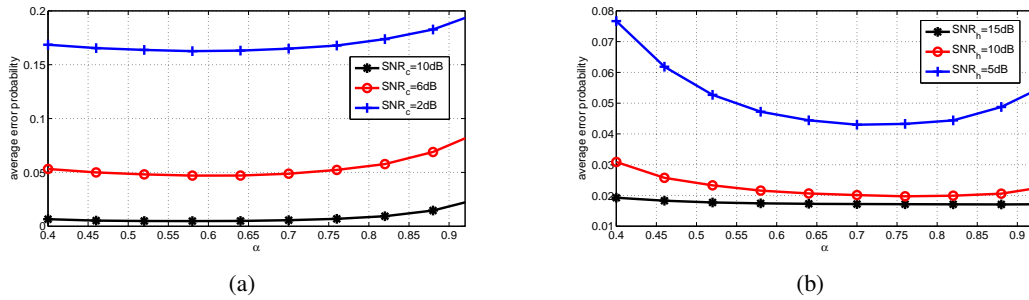


Fig. 4. “STC@sensors”: majority rule (a) $SNR_h=5\text{dB}$ with $SNR_c=2,6,10\text{dB}$ (b) $SNR_c=6\text{dB}$ with $SNR_h=5,10,15\text{dB}$

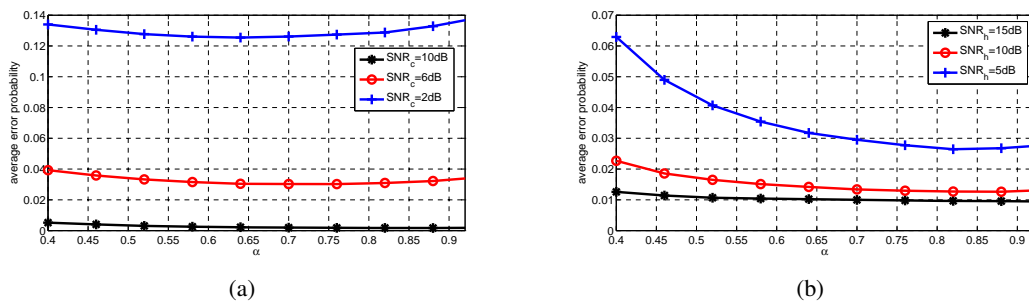


Fig. 5. “fusion@sensors”: majority rule (a) $SNR_h=5\text{dB}$ with $SNR_c=2,6,10\text{dB}$ (b) $SNR_c=6\text{dB}$ with $SNR_h=5,10,15\text{dB}$

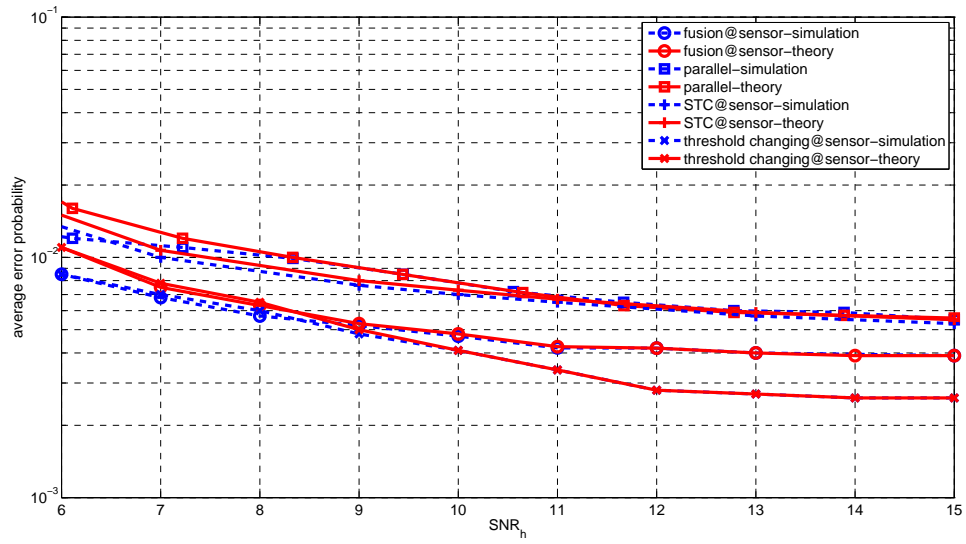


Fig. 6. Monte-Carlo simulation versus analytical results